crystals

MDPI

Review

Carbon-Supported Noble-Metal Nanoparticles for Catalytic Applications—A Review

Agnieszka Karczmarska [1,*], Michał Adamek [1], Sara El Houbbadi [1], Paweł Kowalczyk [2] and Magdalena Laskowska [1,*]

[1] Institute of Nuclear Physics Polish Academy of Sciences, 31-342 Krakow, Poland; michal.adamek@ifj.edu.pl (M.A.); sara.elhoubbadi@ifj.edu.pl (S.E.H.)
[2] Department of Animal Nutrition, The Kielanowski Institute of Animal Physiology and Nutrition, Polish Academy of Sciences, 05-110 Jabłonna, Poland; p.kowalczyk@ifzz.pl
* Correspondence: agnieszka.karczmarska@ifj.edu.pl (A.K.); magdalena.laskowska@ifj.edu.pl (M.L.)

Abstract: Noble-metal nanoparticles (NMNPs), with their outstanding properties, have been arousing the interest of scientists for centuries. Although our knowledge of them is much more significant today, and we can obtain NMNPs in various sizes, shapes, and compositions, our interest in them has not waned. When talking about noble metals, gold, silver, and platinum come to mind first. Still, we cannot forget about elements belonging to the so-called platinum group, such as ruthenium, rhodium, palladium, osmium, and iridium, whose physical and chemical properties are very similar to those of platinum. It makes them highly demanded and widely used in various applications. This review presents current knowledge on the preparation of all noble metals in the form of nanoparticles and their assembling with carbon supports. We focused on the catalytic applications of these materials in the fuel-cell field. Furthermore, the influence of supporting materials on the electrocatalytic activity, stability, and selectivity of noble-metal-based catalysts is discussed.

Keywords: noble-metal nanoparticles; carbon-supported nanoparticles; catalysts; fuel cells

Citation: Karczmarska, A.; Adamek, M.; El Houbbadi, S.; Kowalczyk, P.; Laskowska, M. Carbon-Supported Noble-Metal Nanoparticles for Catalytic Applications—A Review. *Crystals* **2022**, *12*, 584. https://doi.org/10.3390/cryst12050584

Academic Editors: Raghvendra Singh Yadav and Suresh Kannan Balasingam

Received: 22 March 2022
Accepted: 20 April 2022
Published: 22 April 2022

1. Introduction

Not without reason, metals such as gold and silver are referred to by the adjective noble, which means causing admiration for a particular appearance or quality. For centuries, people have valued and used gold and silver for many purposes. These noble metals, known since ancient times, have been frequently used as a means of payment, even before the invention of coins. However, their value was derived from other applications, particularly those related to esthetic and medicinal purposes. Gold, like all precious metals, is resistant to corrosion and oxidation, but is also malleable, ductile, has a natural luster that can be polished to create a shiny appearance, and does not tarnish. These qualities meant that gold was used for special decorative ornaments, jewelry, and religious artifacts [1]. From antiquity to the middle ages, artisans used a mixture of gold salts with molten glass to produce gold colloids with a rich ruby color for coloring glass, ceramics, and pottery. An excellent example of the unique properties of gold nanoparticles dates from the 4th century AD, the famous Lycurgus cup made from glass that appears red in transmitted light and green in reflected light [2]. In addition to the decorative use of gold, its use for medical purposes should be mentioned. All ancient civilizations utilized gold in medicine because of the belief in its immortal nature as a rejuvenating agent, but also as a cure for diseases such as heart and venereal problems, dysentery, epilepsy, and tumors [2,3]. Silver was valued primarily as an antimicrobial and wound-healing agent [4]. Until the Middle Ages, silver was also used as a cure for diseases such as wound infections, epilepsy, or ulcers. In addition, ancient Egyptians, Greeks and Romans used silver vessels to keep water, wine, and food fresh [4]. From the 17th century onwards, systematic research into the chemical

processing of metal ores has taken place, with many discoveries, as presented in a scheme in Figure 1 [4,5].

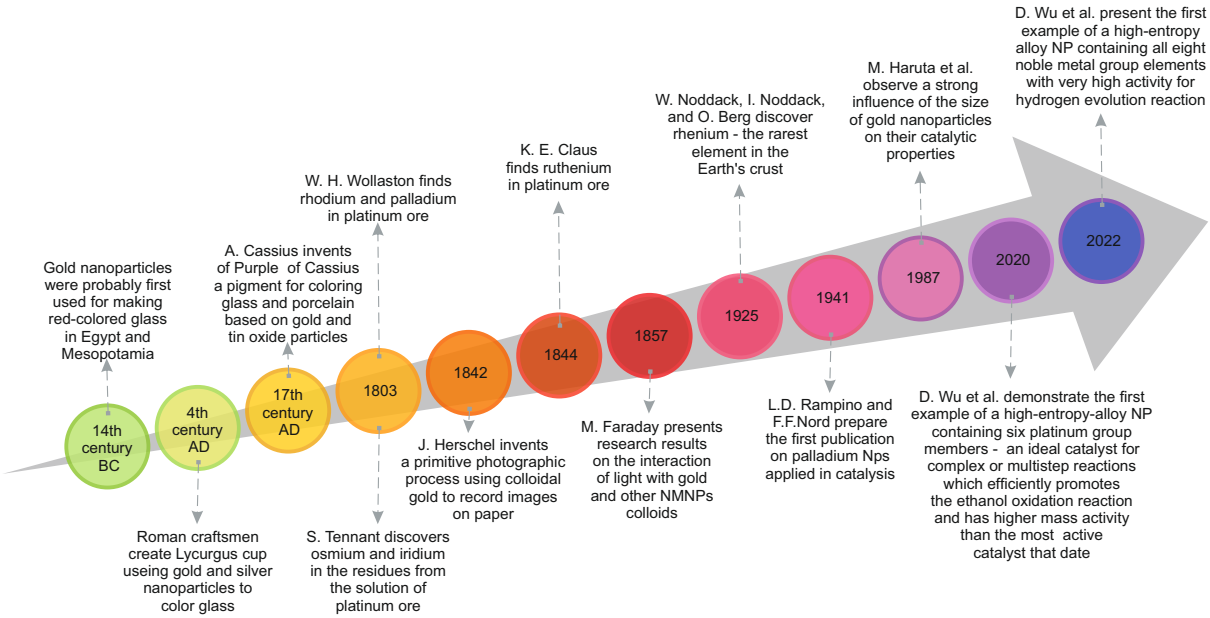

Figure 1. The history of noble metals and their nanoparticles [4–12].

The modern era of NMNPs synthesis began in 1857, when Michael Faraday presented the results of his research on gold and other metal colloids, thin films, and transparent leaves. His research involved gold and other metals, such as silver, platinum, rhodium, palladium, copper, zinc, aluminium, tin, lead, iron, mercury, and antimony, their film formation and interaction with light [6,7]. M. Faraday examined most of the noble metals known at that time.

Noble metals, for centuries, have given immortality to objects made of them, prolonged human lives, and kept the food stored in them in good condition. Today, we are at a point in history where we must again reach for the unique properties of precious metals to return our planet to a good condition. Bearing in mind environmental pollution, global warming, and the current situation of finite fossil-fuel resources, we need to reduce CO_2 emissions and air pollution due to the emissions of SO_x and NO_x and focus on renewable energy sources [13]. We need to find a new way to utilize and store green energy. Many people believe that hydrogen may be the best option. However, is it a new way? The devices for obtaining hydrogen and fuel cells utilizing it as fuel have been known for over a century, and indeed, they seem to be good candidates to replace fossil fuels and internal-combustion engines. Then why did it not happen that these technologies have been used? In the early stage of fuel-cell development, at the beginning of the 20th century, the widespread availability of fossil fuels made the use of fuel cells economically unreasonable.

Nevertheless, fuel cells have many advantages. Above all, they convert chemical energy directly to electrical energy by electrochemical reactions. Their theoretical conversion efficiency is very high compared to heat engines [14]. They have no moving parts, so they are very quiet. It should also be mentioned that fuel cells are zero-emission environmentally friendly technology with water as a waste product. An additional advantage of this technology is its flexibility, which makes fuel cells suitable for various applications. They are suitable for both mobile and stationary devices and can power large vehicles as well as small phones [15]. Despite all the advantages, they are not widely used, mainly for economic reasons. One of the most significant barriers for the widespread commercialization of fuel cells and unitized-regenerative-fuel cells (URFC) is the high cost of their production, which requires a precious Pt electrocatalyst [16,17]. Intensive research for solutions leading to reducing their production costs is constantly ongoing. Among the possible solutions to

reduce the cost of these devices is a reduction in the amount of the noble metal electrocatalyst, which can be achieved by reducing the size of the particles, combining them with other metals into alloys, and modifying the shape of the particles. Another way is using a high-surface-area support to enhance the dispersion of metal nanoparticles and thus to increase the utilization and efficiency of the precious metal electrocatalyst [18].

This article reviews the recent progress of research on carbon-supported noble-metal NPs assembly for catalytic application in fuel-cell technologies. With that in mind, we will highlight, in this article, the current state of knowledge in the field of fuel cells and hydrogen-based energy technology in general. We also want to show the progress that has been made in the area of the synthesis of NMNPs in recent years, which manifests in a number of synthesis methods as well as a variety of obtained nanoparticles. Finally, the heterogenization of noble metals on carbon supports will be discussed.

2. Hydrogen-Based Energy Technology

Fuel cells are highly effective electrochemical devices that dynamically convert chemical energy into electrical energy, which have been known for over 180 years. In 1838, the main concept of the fuel cell was presented by William Robert Grove. He used two platinum electrodes with one end of each immersed in a solution of sulphuric acid, and the other ends separately sealed in containers of oxygen and hydrogen, and he observed that a constant current flowed between the electrodes [19]. It was the first hydrogen fuel cell, called a "gas battery," because it was built by combining several sets of these electrodes in a series circuit. A schematic illustration of Grove's "gas battery" powering an electrolyser is shown in Figure 2. Generally, fuel cells work just like batteries, converting chemical energy directly to electrical energy, but they produce electricity from an external supply of fuel and an oxidant, so they can work constantly. The inverse process to the one occurring in the hydrogen fuel cell was observed by Anthony Carlisle and William Nicholson three decades before Grove's experiment. It was the first observed electrochemical reaction, which relied on the decomposition of water into hydrogen and oxygen using electricity [20].

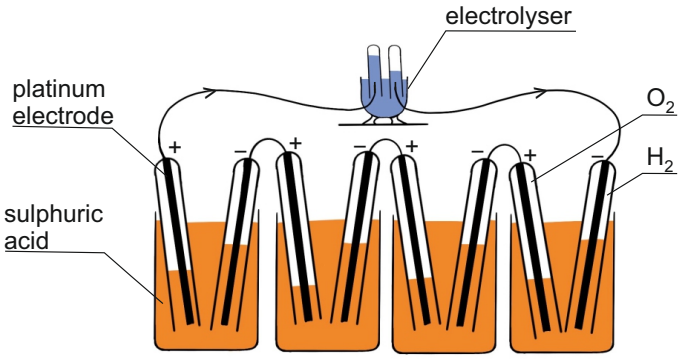

Figure 2. Grove's gas battery powering an electrolyser.

A fuel cell can be combined with an electrolyser, which is a hydrogen generation device, to constitute a system often called a regenerative fuel cell (RFC) or unitized-regenerative fuel cell (URFC). This technology enables hydrogen production using green energy to reduce the effects of intermittency associated with daily and seasonal fluctuations in sunlight and wind availability [13]. This technology allows for the more efficient and stable operation of wind and solar power plants, which are strictly dependent on weather conditions.

When writing about the early history of fuel cells, it is important to mention the crucial role of Friedrich Wilhelm Ostwald, who is considered as the founder of chemistry–physics. His pioneering work in 1893 concerning the chemistry of fuel cells was the basis for further research in this field. In this work, he presented an experimental determination of the proper interconnection of a fuel cell's components and a theoretical understanding of its roles [21,22]. The 20th century was a time of intense research on the complete explanation and optimization of electrodes, electrolyte, oxidizing and reducing agents, anions, and cations' roles and properties. In its results, many types of fuel cells were developed. Among

them, we can distinguish many types according to the operating temperature, electrolyte type (a polymer–electrolyte membrane, also called a proton-exchange membrane fuel cell (PEMFC), alkaline fuel cell (AFC), molten-carbonate fuel cell (MCFC), solid-oxide fuel cell (SOFC) ect.) [14] or type of fuel (hydrogen [23], hydrocarbons [24], alcohols [25], etc.).

Nowadays, one of the most promising fuel cell types is the proton-exchange membrane fuel cell (PEMFC). This technology currently gives the best chance for a quick reduction in production costs and, thus, for widespread commercialization [26]. There are numerous advantages of this technology, such as high power density, low-temperature operation (under 90 °C), a compact system, fast start up, and ease in handling liquid fuel [27]. These are the reasons why this type of fuel cell has found many applications. PEMFCs are excellent electrical-power sources for vehicles and portable applications such as phones, but also for large-scale power generation [15].

The very high production costs of fuel cells and difficulties in reducing them result directly from fuel-cell construction. Figure 3 shows the essential components in a PEM fuel cell, with its central component membrane-electrode assembly (MEA), which consists of an electrolyte sandwiched between electrodes—an anode and a cathode. The electrodes provide the flow of current by an external circuit and, at the same time, serve as an electrocatalyst. The anode is the electrode on the fuel side where the hydrogen oxidation reaction (HOR) occurs, while the cathode is the electrode on the air side where the oxygen-reduction reaction (ORR) takes place. The electrolyte serves as a barrier to gas diffusion but allows ions migration across it [28]. The cathode and anode reactions for PEM supplied by pure hydrogen are the following:

Anode:

$$H_2 \rightarrow 2H^+ + 2e^- \quad (1)$$

Cathode:

$$\frac{1}{2}O_2 + 2H^+ + 2e^- \rightarrow H_2O \quad (2)$$

The simplest and most common fuel for the PEMFC is hydrogen. It can be delivered to the cell in the form of a pure gas stream or in the form of a reformate produced from various fuels, such as methane, methanol, or petrol. Among PEMFCs, we can also find cells supplied directly by alcohols. Examples of these cells are called the direct methanol fuel cell (DMFC) and the direct ethanol fuel cell (DEFC). In these fuel cells, a methanol-oxidation reaction (MOR) and an ethanol-oxidation reaction (EOR) occur [29]. For a DMFC, the cathode and anode reactions can be written as follows [30]:

Anode:

$$CH_3OH + H_2O \rightarrow CO_2 + 6H^+ + 6e^- \quad (3)$$

Cathode:

$$\frac{3}{2}O_2 + 6H^+ + 6e^- \rightarrow 3H_2O \quad (4)$$

In both cases, these reactions need catalysts to increase the rate of the particular reactions occurring on the anode and cathode, which leads to reducing the electrochemical over-potential and increasing the voltage output [31].

The requirement for precious metals as electrocatalysts is one reason for the high production costs. The other reasons arise from the specific requirements for individual membrane-electrode assembly (MEA) components. Intensive work is still underway to improve power densities and reduce operative costs at the same time. On the one hand, researchers are focused on reaching a proton-exchange membrane with high proton conductivity, low electronic conductivity, low permeability to fuel, a low electroosmotic drag coefficient, high chemical and thermal stability, good mechanical properties, and of course, a low cost [32]. On the other hand, work is underway to develop the optimal electrode, which must meet three conditions: (i) be able to transport gaseous or liquid species, (ii) be able to transport ions, and (iii) be able to transport electrons to rapidly catalyze electro-oxidation (anode) or electroreduction (cathode) [28]. To meet these requirements, the electrode must be electronically and ionically conducting, electrochemically active, porous,

and have a high surface area, which is hard to fulfill by one material. Therefore, most cathodes are made of composite materials and one of the components is an electrocatalyst. The typical PEMFC needs Pt-based electrocatalysts for both the anodic hydrogen-oxidation reaction and the cathodic oxygen-reduction reaction [26].

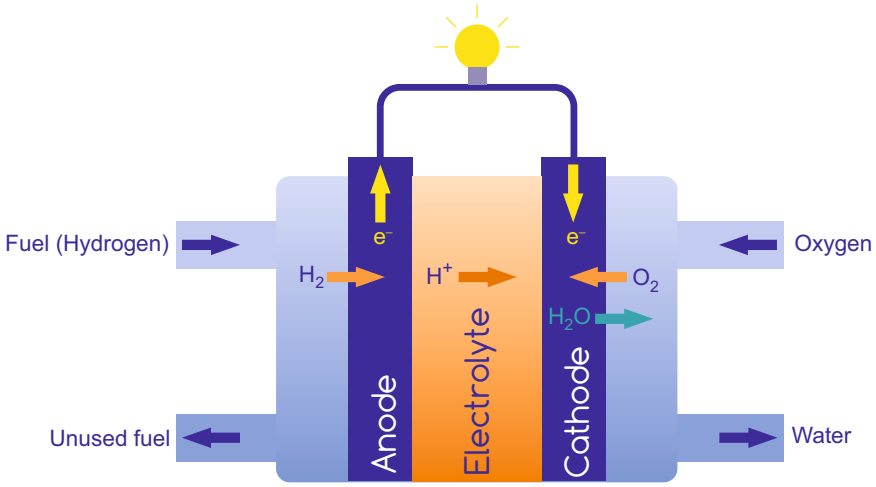

Figure 3. Scheme of hydrogen fuel cell.

Generally, Pt-based electrocatalysts are utilized. The anode requires a low Pt loading due to its fast hydrogen-oxidation reaction (HOR) kinetics, but the cathode requires a much more efficient and durable electrocatalyst. The kinetics of the oxygen-reduction reaction (ORR) that occurs on the cathode is much slower than the HOR. The sluggish kinetics of the reaction on the cathode, which is around five orders of magnitude lower than for the reaction on the anode, often demand better electrocatalysts than pure platinum [26]. Beermann et al. point to the necessity to create nanoparticle catalysts based on alloying platinum with transition metals (e.g., Fe, Co, Ni, Cu) [33]. Especially promising electrocatalysts can be high-entropy alloys (HEAs) with less than 50 at.% Pt that can maintain high-ORR activity and stability in various environments [34]. An excellent example of an HEA nanoparticle, presented by Wu et al., is a nanoparticle that consists of all the platinum group members, which can be an efficient catalyst for complex or multistep reactions [12]. However, catalytic activity is not the only challenge. Another challenging task is the durability of the catalysts used in fuel cells.

Numerous authors point out the difficulties of maintaining a constant high-electrochemical performance. Among the potential degradation mechanisms, they mention carbon corrosion, particle detachment, Ostwald ripening, particle migration, which can lead to agglomeration or coalescence, and platinum dissolution (Figure 4) [35,36]. In Section 4, the methods that can be implemented to eliminate degradation mechanisms through the appropriate selection of the carbon supports or the method of immobilizing nanoparticles on the carbon support will be analyzed.

Another challenge facing researchers is the high cost of platinum, which is the main reason for very high operating costs. Therefore many efforts have been made to reduce the costs associated with the use of precious metals as electrocatalysts. Among the different approaches proposed are a reduction in Pt loadings, the use of less expensive noble metals such as Pd and Ru, and the development of alternative low-cost electrocatalysts based on non-noble metals and molecular chemistry [37]. Many studies also indicate the significant impact of the carbon substrate as a carrier of NMNPs on their catalytic activity. Therefore, in the following parts of this article, particular types of carbon substrates and their influence on the catalytic properties of NMNPs will be discussed.

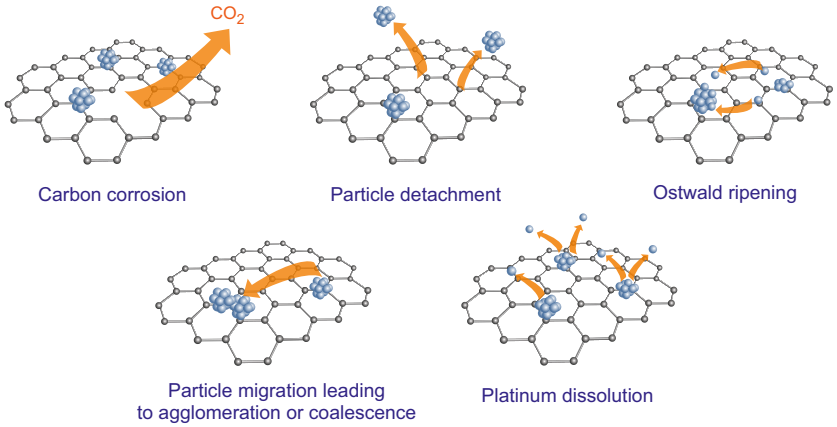

Figure 4. The degradation mechanisms of carbon-supported NMNPs catalysts.

3. Synthesis of Noble-Metal Nanoparticles

Historically, the first method described was that used by Michael Faraday. He prepared his colloidal dispersions of gold by a process of reducing an aqueous solution of a gold salt, such as sodium tetrachloroaurate ($Na[AuCl_4]$), with a solution of phosphorus in carbon disulfide. At room temperature, this reaction proceeds very quickly and the light yellow colour of the $Na[AuCl_4]$ solution changes within a few minutes to the ruby-red colour typical of colloidal gold [38]. Since then, many various synthesis procedures have been developed and described in thousands of publications.

Generally, the procedures of obtaining noble-metal nanoparticles can be divided into two groups: the bottom-up and top-down approaches. The bottom-up method is the most frequently used approach in the synthesis of nanoparticles because it gives many advantages, such as the ability to obtain monodispersity and precisely controlled particle size and structure. This method involves building up material from the bottom: atom by atom or molecule by molecule. Top-down approaches depend on the partitioning of bulk materials (milling, sputtering, pyrolysis, laser ablation) or on the miniaturization of production processes to produce the desired structure with the appropriate size and properties (lithography). This method is simpler but has many disadvantages and limitations, one of which is the inability to control particle size and structure. In addition, this method causes imperfections in the surface structure, which significantly affects the physical and chemical properties of the resulting nanoparticles.

Another distinction of noble-metal NPs preparation methods could be the division between chemical and physical methods. The chemical methods include chemical reduction using a reducing agent [39,40], the electrochemical method [41,42], the sonochemical method [43,44] and green synthesis [45,46]. The physical methods comprise of pyrolysis [47,48], nanolithography [49,50], thermolysis [51] and radiation-induced methods [52,53]. Physical methods usually require special equipment, so they are infrequently available. Therefore, in this review, we will describe simple chemical methods that can be repeated in an averagely equipped laboratory.

The most frequently applied and reliable method of NMNPs synthesis is chemical reduction [54]. This reaction includes the reduction of a precursor dissolved in a solvent by reducing agents and stabilization, as presented in Figure 5. As reducing agents, borohydrides, aminoboranes, hydrogen, acetylene, formaldehyde, hydrazine, hydroxylamine, polyols, citric and oxalic acids, sugars, hydrogen peroxide, carbon monoxide, sulfites can be used and other electronic reducing agents including electron-rich transition-metal sandwich complexes [55]. The choice of reductant is dictated by the conditions in which the reaction is carried out because the activity of reducing agents is strongly conditioned by the pH of the solution [56]. Among inorganic reductants, alkali metals borohydrides, such as sodiumborohydride ($NaBH_4$), are powerful reagents and they represent a historical cornerstone in the list of such compounds. Sodiumborohydride is one of the most powerful inorganic reductants, which is suitable to reduce cations of noble metals such as gold [57],

silver [58,59], platinum [60], palladium [61], rhodium [62], ruthenium [63], osmium [64], iridium [65], to their nanosized elemental state, according to the equation below [56]:

$$n\mathrm{BH}_4^- + 8\mathrm{Me}^{n+} + 8\mathrm{nOH}^- \rightarrow n\mathrm{BO}_2^- + 8\mathrm{Me} + 6\mathrm{nH}_2\mathrm{O} \quad (5)$$

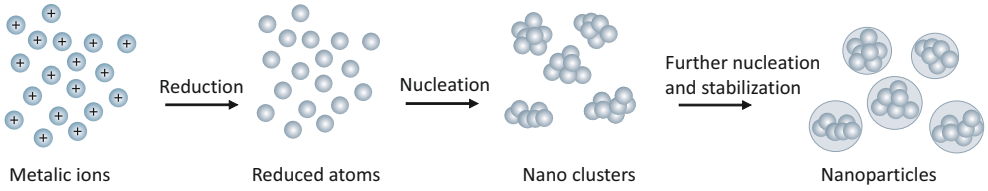

Figure 5. Reduction of metal ions in solution.

An example of a simple and efficient method for the synthesis of NMNPs with controlled size and shape is the chemical reduction of the metallic precursor in the presence of a capping agent. The first shape-controlled colloid–chemical synthesis of Pt nanoparticles used the hydrogen reduction of potassium tetrachloroplatinate(II) (K_2PtCl_4) in the presence of sodium polyacrylate (NaPA) [66–68]. Similar reduction techniques have been used by several other authors to prepare differently shaped noble-metal nanocrystals in the presence of a number of other capping agents, for example, surfactants (e.g., CTAB, SDS) [69–72], polymers (e.g., PVP, PVA) [73,74], and ligands (e.g., inorganic ions, thiols, amines) [75]. These additives, present in the reaction medium, play important roles in controlling the morphology of particles produced. Capping agents interacting with particle surfaces can significantly change the growth rate of the NPs, inhibiting the incorporation rate of growth units onto the particle surfaces and changing the surface free energies of different facets [71,76,77]. Unfortunately, surfactants, as organic molecules deposited on the surface of NPs, can block the catalytic active sites and prevent the use of such nanoparticles in catalytic processes. Therefore, it is necessary to use effective methods of removing surfactants without disturbing the shape of NPs before their application as catalysts [78,79].

Another frequently used method is the seed-mediated growth method. A popular example of its use is the synthesis of Au nanorods, but other shapes can also be achieved using this method [80]. Gold nanorods could be synthesized by adding small Au seeds into a growth solution containing a gold (III) chloride solution ($HAuCl_4$), silver nitrate ($AgNO_3$), ascorbic acid (AA) and cetyltrimethylammonium bromide (CTAB). The acid reduces Au^{3+} to Au^+, and the addition of seeds catalyzes the reduction of Au^+ to Au^0, leading to the generation of Au nanorods [80–82].

The synthesis of NMNPs with the ability to control size and shape has attracted the wide attention of researchers because of the strong relation between structure and catalytic performance [83–85].It is well-known today that size, shape, and morphology determine the catalytic properties of NMNPs since the catalytic performance directly depends on the distribution of atoms on the nanoparticle surface [86–88]. A higher NMNPs mass activity, i.e., the catalytic activity per given mass of nanoparticles, should be achieved. This will reduce the required consumption of noble metals in fuel cells. To date, the highest specific activities (normalized by surface area) have generally been achieved on single-crystal surfaces or well-defined platinum nanoparticles and its alloys with specifically engineered facet structure [84,88]. One of the first reports on the influence of nanoparticle size on their catalytic properties was the work of Haruta et al. in 1987 [10]. They claimed that size plays a crucial role in enhancing gold nanoparticles' catalytic activity. Gold NPs with a 5 nm diameter were not only much more active but also were much more stable than the conventional catalyst. In the same publication, the authors also drew attention to the proper selection of the support for nanoparticles and their role in the catalytic process, presenting the results for three different metal oxides as supports for gold nanoparticles.

One of the parameters that depends on the nanoparticle diameter is its specific surface area, which is the key parameter in catalysis. Some research focuses on increasing

the surface of catalysts not only by decreasing the diameter but also by forming porous particles [89], stars [90], or frames [91].

Chemical composition is another critical factor that affects the catalytic activity of nanoparticles. Over the years, methods to create multimetallic nanoparticles such as bi- [92,93] or three-metallic [94–96] NPs have been developed. Especially, alloy materials exhibit various mechanical and chemical properties not observed for single-component NPs. Thus, designing alloy NPs seems to be a promising way for new catalyst preparation. Among different alloy NPs, high-entropy alloys (HEAs) are attracting much attention. It should be mentioned that the first HEA nanoparticle containing six platinum group members was demonstrated by D. Wu et al. in 2020. One year later, D. Wu et al. presented the first example of a high-entropy-alloy NP containing all eight noble-metal-group elements. Designing precisely tailored HEA NPs is the most promising direction for the further development of catalytic nanomaterials [8,12].

In summary, by using simple chemical methods, numerous researchers have succeeded in synthesizing a variety of nanoparticles with different shapes for specific applications (spheres, octahedrons, cubes, cuboids, rods, wires, decahedrons, icosahedrons, and wafers) [97,98]. Table 1 shows the variety of NMNPs obtained by the simplest reduction method and summarizes the procedures for the synthesis of noble-metal NPs depending on the type, size and shape of the nanoparticles obtained.

Table 1. Examples of NMNPs with different shapes and sizes along with reagents used to synthesize them.

Metal	Shape	Size [nm]	Precursor	Reductant	Stabilizer	References
Au	Spherical	20–50	$HAuCl_4$	SC	-	[99]
	Spherical	3.5–4	$HAuCl_4$	$NaBH_4$	SC	[100]
	Nanoprisms	144 ± 30 (edge length)	$HAuCl_4$	$NaBH_4$	CTAB and AA	[101]
	Nanostars	37 ± 2	$HAuCl_4$	HEPES	PVP	[102]
Ag	Cubic	18–32	CF_3COOAg	DEG	PVP	[103]
	Nanorods	80–100 (diameter)	$AgNO_3$	EG	PVP	[104]
	Nanostars	~300	$AgNO_3$	HA	CCA	[105]
	Flower-like	~450	$AgNO_3$	CCA	CTAB	[106]
	Spherical	10–200 (tunable)	$AgNO_3$	SC and TA	-	[107]
Pt	Spherical	4.9	H_2PtCl_6/K_2PtCl_4	$NaBH_4$	PEI	[108]
	Cubic Tetrahedral	5.2	H_2PtCl_6/K_2PtCl_4	$NaBH_4$	PEI	[108]
	Spherical Tetrahedral Octahedral (tunable)	3–30	H_2PtCl_6	EG	PVP	[109]
Pd	Spherical	5–15	$PdCl_2$	TEG	PVP	[110]
	Nanodendrites	50	Na_2PdCl_4	SA	Phosphonic acids with aromatic side chains	[111]
	Spherical	1.5–23.3 (tunable)	$PdCl_2$	$NaBH_4$	PVP	[112]
Rh	Spherical	1.5–4	$Rh(acac)(CO)_2$	-	PVP/PVA	[113]
	Spherical	2.9–5.6	$RhCl_3$	$NaBH_4$	PEG-tagged imidazolium salts	[114]
	Triangular	10	$RhCl_3$	TREG	PVP	[115]
Ru	Pompon-like	~148	$RuCl_3$	TREG	PVP	[116]
	Spherical	1.4–7.4	$RuCl_3$	EG/DEG/TEG	PVP	[117]
	Cubic	2.4–5	$Ru(acac)_3/RuCl_3$	EG/TEG	PVP	[118]
Ir	Spherical	2.5 ± 0.5	$IrCl_3$	$NaBH_4$	SC	[119]
	Spherical	~3	H_2IrCl_6	EG	-	[120]
	Spherical	3–4	$IrCl_3$	$NaBH_4$	TA	[65]
Os	Spherical NPs forming nanochains	1–1.5 (single NP)	$OsCl_3$	AA	AA	[121]
	Cubic	0.7–1.8	$Os(acac)_3/OsCl_3$	EG	PVP	[122]

4. Carbon-Supported Noble-Metal Nanoparticles

As presented in the previous sections of this article, the numerous physicochemical properties of NMNPs, including optical, catalytic, as well as biological properties, have led to a growing interest in these nanomaterials in laboratories in recent years [97,123,124]. Gold and silver nanoparticles, due to their optical properties which are related to the existence of localized surface plasmon resonance (LSPR), are used in highly sensitive analytical methods such as surface enhanced Raman spectroscopy (SERS) [125,126] for biolomedical applications [127,128]. Biological properties, including the high antibacterial activity of NMNPs, have made them very attractive in nanotechnology and medicine [129,130]. For years, Pt-based nanostructures have been widely used to obtain various types of catalysts [131–133]. Among the unique properties used for fuel-cell applications are the catalytic activity, selectivity and stability of the nanocomposites [134]. The catalytic processes are localized on the surface of the particles, so their efficiency is directly related to their morphology, size and shape, and composition [135,136]. By reducing the particle size, a greater specific surface area (SSA) is achieved, as well as more active catalytic sites, resulting in higher electrocatalytic activity [137]. Despite the great progress in the synthesis of new noble metal nanoparticles, there are still some difficulties in their application in catalytic processes. Besides the low yield and high cost of the syntheses, issues of their agglomeration under conventional catalytic-reaction conditions remain [138–140]. Therefore, work has begun on integrating them with other stable and inexpensive materials, which have helped to optimize their properties and minimize their consumption [141–144]. The resulting compositions not only possess the combined properties of the individual components, but also potentially exhibit new functions and enhanced performance [145–147]. The support provides NMNPs with a higher surface-area-to-volume ratio, contributing to the increased catalytically active areas in which reactions occur [148,149].

To date, noble-metal nanoparticles have been successfully incorporated with polymers [150–152], oxides (e.g., SiO_2 [153], Al_2O_3, TiO_2 and CeO_2 [154] Nb_2O_5, Ta_2O_5, and ZrO_2 [155]), metal–organic frameworks (e.g., ZIF-8, MIL-101-NH2) [156,157] and carbon materials (e.g., carbon black, carbon nanotubes, graphene) [158–161]. Over the past decades, carbon materials have been recognized as an ideal substrate because of their extraordinary physical and chemical properties and their universal availability, processibility, environmental friendliness, and relative stability in both acidic and basic media [162]. At this point, it should be added that carbonaceous materials (CMs) have a large specific surface area, high porosity, excellent electron conductivity, relative chemical inertness, good thermal stability under an inert atmosphere, an intrinsic hydrophobic nature, and the presence of vast functional groups that facilitate metal loading [159,163].

Depending on distinct types of crystal structures, carbon atoms can form a variety of allotropes with different properties [164]. In particular, carbon nanomaterials, such as 0D fullerenes, 1D carbon nanotubes, 2D graphene, etc., have dynamized research in the field of electrocatalysis. Built on them, NMNPs/CMs nanocomposites are an ideal option for various electrochemical reactions in energy conversion and storage, including hydrogen evolution and oxygen reduction. These materials withstand various types of electrochemical oxidation reactions, which reduce the lifetime of electrocatalysts due to sintering and poisoning effects [165,166].

In conventional systems, carbon black, which is a product produced by the pyrolysis of petroleum hydrocarbons, is usually used as a carrier for Pt nanoparticles. Due to its high availability and low cost, it is widely used in electrocatalysis applications [167]. Common carbon blacks include acetylene black, Vulcan XC-72, Ketjen Black, etc. Their major physicochemical characteristics include specific surface area, electronic conductivity, large surface-to-volume ratio, stability, and surface functionality [168–172].

4.1. Methods of Obtaining NMNPs/CMs Nanocomposites

Thus far, a lot of work has been devoted to developing new, efficient methods for the preparation of electrochemically active NMNPs/CMs nanocomposites. It was found that

the smaller and more homogeneous the immobilized metal particles are, the better the electrocatalytic properties of the nanohybrid [173–175]. Among the chemical-deposition methods of NMNPs on carbonaceous supports, one can distinguish: surface-functionalization methods, electrochemical deposition, and electroless deposition [176,177]. In this work, it has been decided that detailed descriptions of the syntheses of nanocomposites and their catalytic properties are to be presented for the most frequently described, i.e., widely understood, mesoporous carbon materials, carbon nanotubes, and graphene (Figure 6). Examples of other carbon supports along with an indication of the synthesis method are summarized in Table 2.

Table 2. Examples of carbon-supported nanocomposites categorized by synthesis method.

Synthesis Method	Precursors	Type of NMNPs	NM Particle Size [nm]	References
Surface functionalization	CNF, NaOH, H_2SO_4, H_2PtCl_6	Pt	6	[178]
	CNF/TiO_2, EG, NaOH, H_2PtCl_6	Pt	3.8	[179]
	Ketjen Black, HNO_3, H_2PtCl_6	Pt	2.5	[180]
	N-CNT, HCOOH, H_2PtCl_6	Pt (nanorods)	3–4 × 10	[181]
	Vulcan XC72, HNO_3, H_2PtCl_6	Pt	2.2 ± 0.4	[182]
	rGO, HCOOH, H_2PtCl_6, $PdCl_2$	PtPd	4 × 20–200	[183]
		Pt nanowires	5	
		Pd nanoparticles		
	Ni-N-CNTs, PDDA, $PdCl_2$	Pd	2–5	[184]
	MWCNTs, THF, H_2PtCl_6, $SnCl_4$	PtSn	~4	[185]
	CX, HNO_3, H_2PtCl_6, $RuCl_3$	PtRu	3.8-4.4	[186]
	BDD, NaOH, SDBS, $RuCl_3$, H_2PtCl_6	PtRu	2–5	[187]
	rGO, $KAuCl_4$, K_2PtCl_6	Pt	2.34 ± 0.52	[188]
		Pt-Au	2.86 ± 1.30	
	rGO, Vulcan XC-72, H_2PtCl_6	Pt	0.5–2.5	[189]
	G - CNTs, KOH, H_2PtCl_6	Pt	4.3–6.8	[190]
	rGO, EG, $HAuCl_4$, H_2PtCl_6	Pt-Au		[191]
	CQD, Vulcan XC-72, H_2PtCl_6, $NaBH_4$	Pt		[192]
	N-GQD, Na_2CO_3, HCl, $PdCl_2$	Pd		[193]
	N-GN, $CoCl_2$, $RuCl_3$	RuCo	6.2	[194]
	C60, H_2PtCl_6,	Pt	<5	[195]
	C60, NaOH, H_2PtCl_6	Pt	3.93–4.20	[196]
	GO-PyrC60, $PdCl_2$	Pd	10	[197]
	CA, Vulcan XC-72R, H_2PtCl_6, $NaBH_4$	Pt	3.24	[198]
	MNC, CCA, NaOH, H_2PtCl_6, $NaBH_4$	Pt	3.1	[199]
	Vulcan XC-72R, NaOH, H_2PtCl_6, H_2IrCl_6	PtIr	3.6–3.9	[200]
	CNT, H_2SO_4, $IrCl_3$	Ir	~1	[201]
	MWCNT, EG, HNO_3, H_2SO_4, H_2PtCl_6, $RuCl_3$, $ReCl_3$	Pt-Ru	2.79 ± 0.58	[202]
		Pt-Re	3.53 ± 0.80	
		Pt-Ru-Re	2.88 ± 0.64	
		Pt-Ru-Re	2.68 ± 0.55	
		Pt-Ru-Re	3.19 ± 0.54	
Electrochemical deposition	CNT, EG, H_2PtCl_6, $RuCl_3$	Pt-Ru	3.1–5.6	[203]
	GO, H_2PtCl_6, KH_2PO_4	Pt	10	[204]
	GO, CNF, H_2PtCl_6, H_2SO_4	Pt	350–500	[205]
	CP, H_2PtCl_6, $RuCl_3$, HCl, KOH	Pt-Ru	52.9 ± 9.2	[206]
	GR, ZnO, K_2PtCl_6, H_2SO_4	Pt	250	[207]
	BDD, $NaBH_4$, NaOH, H_2PtCl_6	Pt	15 ± 5	[208]
	BDD, $Ni(NO_3)_2$, HCl, $PdCl_2$	Pd	~13	[209]
	Vulcan XC-72, H_2PtCl_6, H_2SO_4	Pt	1–4	[210]
Electroless deposition	CNO, H_2PtCl_6	Pt	20	[211]
	CNT, $CoCl_2$, H_2PtCl_6	Pt	30–40	[212]
	CNT, SDS, EG, Na_2PdCl_4	Pd	2–5	[213]
	MWCNT, $HAuCl_4$	Au	10	[214]
	PC, $C_6H_5K_3O_7$, $RhCl_3$, $RuCl_3$, $IrCl_3$	Ir	0.96 ± 0.13	[215]
		Rh	1.11 ± 0.31	
		Ru	1.37 ± 0.39	
	NiO/Ni/CNTs, K_2PtCl_6	Pt	~2	[216]

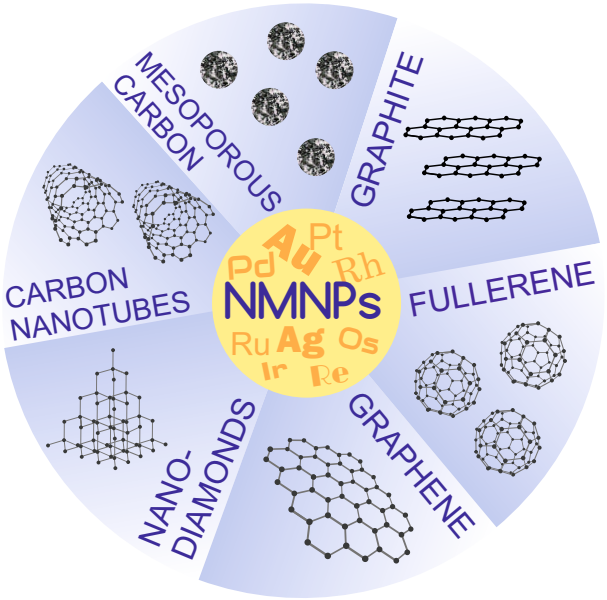

Figure 6. A schematic representation of various carbon supports for NMNPs.

Two types of procedures can be used depending on the requirement. In type 1: previously synthesized metal nanoparticles are deposited on carbon substrates. In type 2: the formation of nanoparticles and their deposition on carbon substrates occurs during a single process. These two processes can be based on the creation of covalent or noncovalent interactions between individual elements of nanocomponents. Both functionalization processes serve to enhance the number of active binding sites for the deposition of metal-nanoparticle catalysts and also to improve the dispersibility of the carbon substrate in water or solvents. These aspects ultimately enhance the catalytic effect [217,218]. In the case of noncovalent functionalization, the hybridization of the material in question remains unchanged. It also has little effect on its electronic properties, as a result of the weak van der Waals forces of attraction between the adsorbates and carbon substrates [176,177,219]. In the case of covalent functionalization, different types of binding sites are generated. One form of covalent functionalization is oxidative means, during which oxygen groups such as carboxyl, carbonyl and hydroxyl groups, are formed [177,220]. They stabilize the dispersion of carbonaceous materials in polar solvents and provide active sites for metal adsorption. Such functionalized carbon materials with noble metal precursors can be further reduced by the addition of reducing agents (e.g., ethylene glycol (EG), $NaBH_4$, H_2, formic acid (HCOOH), etc.) to form NMNPs/CMs hybrids [221,222]. The synthesis process can be significantly accelerated by using an irradiation-assisted technique, for example, visible light or microwave irradiation [223,224]. Particularly noteworthy is the microwave-assisted polyol method, which has numerous advantages such as ease of procedure, speed and safety [225,226].

In the electrochemical method, the MNNPs/CMs nanocompounds are obtained via the reduction of noble metal complexes, such as $H[AuCl_4]$, $H_2[PtCl_4]$, or $(NH_4)_2[PdCl_4]$, by electrons. It consists of the following steps: deposition of carbon material on the electrode, immersion of the carbon-coated electrode in an electrolytic solution containing metallic precursors, and application of an electrochemical potential. Carbonaceous materials act as molecular conductors to provide support for the deposited NMNPs. It should be noted that, in this case, CMs do not react with noble metal salts. The nucleation process and subsequent growth of NPs can be effectively controlled by adjusting electrodeposition parameters such as nucleation potential, deposition time, metal salt concentration, etc. [176, 177,204,206,227,228].

The electrodeless deposition method constitutes a chemical process involving a direct redox reaction, by electron transfer between metal ions (higher reducing potential), and a

carbon support [229,230]. Due to the fact that such a process does not require any external reducing agents, electrodeless deposition is considered as a green strategy for producing metal NPs on carbon substrates [231].

4.1.1. Noble-Metal Nanoparticles on Mesoporous Carbon Materials

Carbon materials with mesoporous characteristics (2 nm < pore sizes < 50 nm) have received considerable attention in electrocatalytic applications. They can facilitate the transport of reactants to the electrocatalysts and simultaneously exhibit large surface areas and low charge-transfer resistance [232–234]. On this basis, numerous examples of the use of mesoporous carbon materials [186,235,236] have attracted much interest as electrocatalyst supports for fuel-cell applications. Using ordered and highly ordered mesopoporous carbon materials as substrates for Pt and PtRu nanoparticles, respectively, it was shown that the size and distribution of mesopores play an important role in electrochemical reactions [236,237]. Qi et al. synthesized PtRu nanoparticles with graphitic mesoporous carbon (GMC) substrates using a chemical reduction process, with H_2PtCl_6 and $RuCl_3$ as precursor nanoparticles [232]. The study involved the use of GMCs with different pore sizes, and the results clearly indicated that this parameter affects the performance of direct methanol fuel cells. Carbon aerogels (CA), which can be synthesized from cellulosic biomass, are another favorable porous material for fuel-cell-energy-storage and conversion applications [238–241]. An example is the work of Gu et al., in which the effect of CA pore size on the deposition of Pt NPs was reported for proton-exchange-membrane-fuel-cell (PEMFC) applications [198]. In the initial stage, CA was impregnated with Vulcan XC-72R carbon, and then platinum nanoparticles (from H_2PtCl_6) were attached to the prepared system by chemical reduction with $NaBH_4$. In turn, Cheng et al. manipulated the potential (potentiostatic deposition or square wave potential deposition) produced Au nanostructures with different sizes and shapes on the surface of carbon fiber paper electrodes [242]. Pt monolayers were deposited onto the resulting urchin-like nanostructures using a surface-limited redox replacement method. The resulting systems were tested in a methanol electrooxidation reaction.

An important step during the synthesis of nanocomposites is the regulation of the surface properties of the MC through different surface-modification methods before the deposition of metal NPs [186,243]. For example, Su et al. deposited uniformly dispersed Pt NPs on the surface of N-doped porous carbon nanospheres (PCNs) [244]. Pt/PCNs hybrids were synthesized by the reduction method using EG as a reducing agent and H_2PtCl_4 as precursor. The process was assisted by microwave irradiation for 3 min. The authors found that Pt/PCNs exhibited increased activity in the methanol oxidation reaction (MOR) than the commercial E-TEK catalyst. In turn, in Ott's group, N-functionalized Ketjen Black carbon powder was used as a substrate for Pt nanoparticles [180]. Modification of the carbon support was carried out by pre-oxidizing the pristine carbon in concentrated HNO_3 at 70, 200, 400 and 600 °C. That modification contributed to the formation of carboxylic, hydroxylic and NO_x groups at the surface and also altered the meso- and microporous structure of the carbon supports. An increase in nitrogen content and a higher proportion of mesopores for media subjected to higher temperatures were observed. Following this, the polyol method was used, in which the carbon and Pt precursor (H_2PtCl_6) were dispersed in ethylene glycol and reduced at 120 °C for 2 h. As a result, Pt NPs were deposited on the outer and inner surface of carbon powder particles, and, thus, a high power density in the fuel-cell catalyst, with high stability under voltage cycling, was obtained.

A parameter that also improves fuel-cell performance is the method of catalyst synthesis [245]. Harzer et al. determined the performance of PEMFC cells depending on the way platinum nanoparticles were distributed on Ketjen Black. Using a polyol method and reducing a highly dilute platinum precursor in ethylene glycol, Pt nanoparticles were obtained on the outer carbon surface and in solution. In contrast, using a prewetting method in which the carbon support is impregnated with a highly concentrated Pt precursor solution,

nanoparticles were obtained inside the pores of the carbon particles. The catalyst with more Pt particles deposited on the outer surface of the carbon achieved better results.

4.1.2. Noble-Metal Nanoparticles on Carbon Nanotubes

Discovered by Iijimain in 1991, carbon nanotubes (CNTs) are one of the most widely used substrates for the formation of NMNPs/CMs complexes. They are defined as the ordered, hollow graphene-based nanomaterials made up of carbon sp^2 - hybridised atoms. They can be classified into the following two categories: (1) single-walled carbon nanotubes (SWCNTs), consisting of a single sheet of carbon that has been rotated into a tubular form, and (2) multi-walled carbon nanotubes (MWCNTs), which are comprised of several concentric SWCNTs having a mutual longitudinal axis [159,246]. The diameter of CNTs is in the nanometer scale, while their length can reach several microns. Numerous examples of NMNPs/CNTs nanohybrids have been reported in the literature for catalytic applications. The first application of NMNPs/CNTs nanocomposites in heterogeneous catalysis dates back to 1994 [247]. This kind of composite material advantageously integrates the unique properties of individual materials and exhibits some innovative features resulting from the interactions between CNTs and NMNPs. These features directly translate into numerous attractive applications in many fields, especially in catalysis, fuel cells, and environmental-contaminant sensing [159,248–251].

Obtaining small size, dispersed particles of noble-metal NPs on CNTs is desirable due to high catalytic activity and also for economic reasons. Despite the fact that CNTs exhibit excellent electrical, mechanical, and thermal properties, however, they are chemically inactive and hydrophobic. As a consequence of this, they often do not have enough binding sites for anchoring guest molecules, which results in low dispersion and a large particle size of nanoparticles. Therefore, functionalization of the external surfaces of CNTs is generally carried out [252]. Preformed NMNPs can be deposited on functionalized CNTs or functionalization and synthesis can be carried out in a single process of the formation of NMNPs/CNTs complexes (Figure 7). The surface modification of carbon nanotubes can be performed either covalently or noncovalently [253]. Such CNTs functionalization methods serve both to increase the number of active binding sites for NMNP deposition and to improve the dispersibility of CNTs in solvents, which enhances the catalytic effects [217,218].

Covalent functionalization of CNTs is often carried out via an aggressive oxidation treatment with a HNO_3 or HNO_3/H_2SO_4 mixture [253]. This process contributes to the formation of several functional groups, such as carboxylic, carbonyl, and hydroxyl groups, on the surface of nanotubes. It can also be carried out by pretreatment of CNTs in HCl, HF, $KMnO_4$ or H_2O_2 [254]. Then, covalently functionalized CNTs often undergo subsequent functionalization processes to control the size and dispersion of the NMNPs deposited on them. That approach was used by Wang's group [255]. In the first step, they functionalized the nanotubes with COOH groups. They then attached amine-terminated ionic liquids (NH_2-IL) to the functionalized nanotubes. The gold salt $[AuCl_4]^-$ was adsorbed to the thus-formed amide bond between MWCNTs-COOH and NH_2-IL through electrostatic interaction and ion exchange. As a result of this process, well dispersed 1–2 nm Au NPs were obtained.

Noncovalent functionalization involves the attraction of the hydrophobic end of an adsorbed molecule to the walls of CNTs via van der Waals forces or π– π interactions [176]. This is carried out without disturbing the electron structure of the CNTs, as the covalent bonds are not affected. In this case, the following may be used aromatic organic compounds such as derivatives of pyrene, thionine, or triphenylphosphine, and they contribute to the formation of several functional groups such as thiol, amine, or carboxyl groups, which can be used as the linkers to anchor NMNPs onto CNTs surfaces. In paper [256], it was shown that, by using the in situ polymerization method, it was possible to obtain a homogeneous polymer coating on the surface of MWCNTs, which allows for better dispersion of the nanotubes. An example of such noncovalent functionalization is the modification of carbon

nanotubes presented by Zheng [257]. The synthesis of Pd/MWCNTs nanocomposites with particle sizes of 3 nm was achieved by π– π stacking interactions of MWCNTs and naphthalen-1-ylmethylphosphonic acid (NYPA).On such functionalized carbon nanotubes, Pd nanoparticles were deposited by means of a homogeneous precipitation–reduction reaction method by using $PdCl_2$ as a noble metal precursor and $NaBH_4$ as a reduction agent.

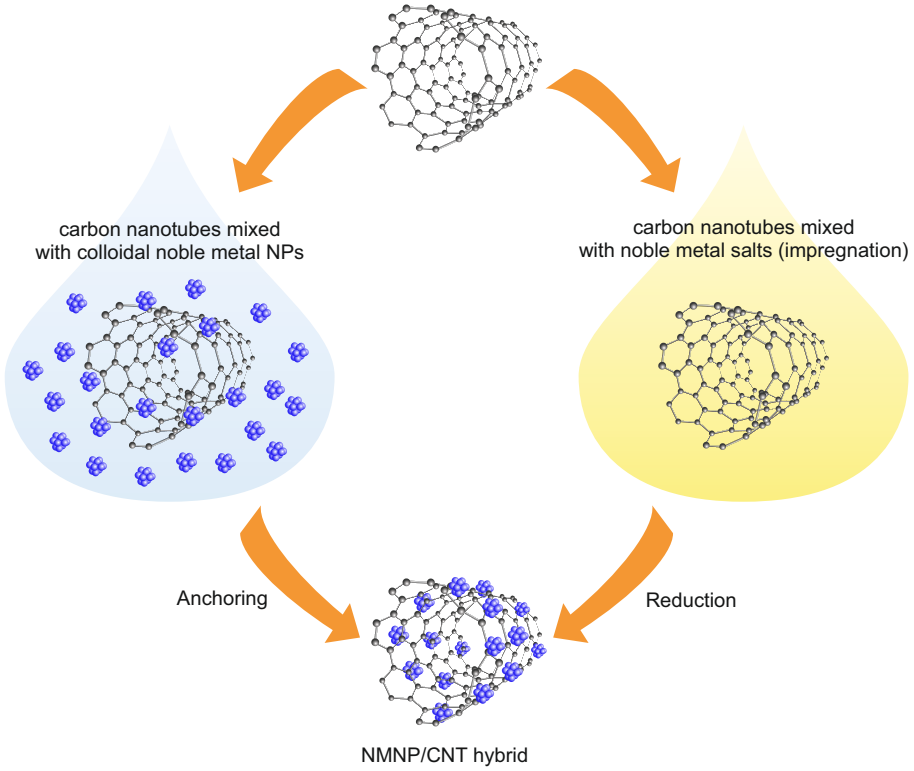

Figure 7. Scheme of the deposition of NMNPs on carbon nanotubes.

Using the same method, it is also possible to form bimetallic-based composites. For example, by reduction with H_2PtCl_6, the addition of ruthenium and molybdenum precursors ($Ru_3(CO)_{12}$, $Mo(CO)_6$), followed by annealing for 2 h at 400 °C in a N_2 atmosphere, bilemetallic Pt-Ru/SWCNTs and Pt-Mo/SWCNTs composites were obtained. Moreover, the as-synthesized Pt-Ru/SWCNTs composite showed better current and power densities than Pt/SWCNTs catalysts [258]. Another bimetallic electrocatalyst that plays an important role in the development of direct-methanol-fuel-cell applications is the PtIr/MWCNTs composite [259].

Another way to improve physical and catalytic properties is doping, realized by replacing the carbon atoms in carbon nanotubes with other elements such as nitrogen, phosphorus or boron. For example, Yu et al. [260] reported doping of MWCNTs with phosphorus (P) and nitrogen (N), which improves their durability and increases their electrocatalytic activity. In turn, Jin et al. reported that Pt/CNTs doped with selenium atoms show long-term stability and good activity in comparison with a commercial Pt/C catalyst [261]. Nitrogen can be used both as a dopant and a surfactant in the growth of CNTs [262]. Nitrogen-functionalized CNTs (N-CNTs) have a high number of surface nucleation sites, which allow the anchorage and high dispersion of the noble metal particles [263]. N-CNTs, as substrate material, possess high resistance to surface oxide corrosion, which is an attractive feature, e.g., in oxygen reduction reactions (ORR) [184]. Noteworthy is also paper [264], which shows that boron doping increases the binding energies of transition metals to CNTs supports more than nitrogen. In turn, Rajala and co-workers fabricated platinum nanowires on SWCNTs (Pt NWs/SWCNTs) then pretreated with ozone, which resulted in the formation of polar surface groups on the carbon nanotubes. The fabricated

Pt NWs/SWCNTs-O_3 composites were more hydrophilic in nature and outperformed in the hydrogen evolution reaction (HER) than non-ozonized compounds [265].

The current trend is the replacement of noble metal nanoparticles in NMNPs/CNTs complexes with cost-effective alternatives, including, for example, nickel. Nickel-doped materials have relatively high electrochemical activity (e.g., ORR, CO_2 reduction) and are low-cost [184]. Zhang et al. developed Pd nanoparticles assembled on Ni- and N-doped carbon nanotubes. The resulting CNTs-based composite with homogeneous and monodispersed Pd and Ni particles (2–5 nm and <1 nm, respectively) achieved much better hydrogen evolution reaction (HER) activity compared with the commercial Pd/C sample.

By using an electrochemical method, a very high purity of nanoparticles and their good adhesion to CNTs substrate can be ensured. However, the NMNPs/CNTs nanocomposites prepared by this method usually receive particles with big particles size (between 10 and 100 nm), as shown in He's work [228]. Pt or bimetallic Pt–Ru nanoparticles were electrodeposited on the CNTs by the potentiostatic method from H_2SO_4 aqueous solution with ruthenium chloride and chloroplatinic acid. The nanoparticles obtained by this method, although characterized by high purity, also had a grain diameter larger than 60 nm. In order to decrease the size of the metal NPs on the CNTs, Tsai et al. [266] synthesized a Pt and a Pt–Ru/CNTs by potentiostatic electrodeposition in mixed sulfuric acid and ethylene glycol containing aqueous electrolytes. It was found that the addition of EG led to the formation of uniformly dispersed and non-agglomerating Pt and Ru NPs with small sizes, ranging from approximately 4.5–9.5 nm and 4.8–5.2 nm for Pt and Pt–Ru, respectively. Grain size reduction can also be achieved by using methods such as cyclic potential scanning [267], pulsed electrodeposition [268], ultrasonic-electrodeposition [269] and a co-electrodeposition/stripping protocol [270].

The formation of NMNPs/CNTs complexes is also possible by using electroless deposition. An example is the use of the one-pot method, which uses a redox reaction between metal ions and reduced CNTs [271]. Using this procedure, Au and Pd NPs were successfully anchored to the surface of MWCNTs and SWCNTs. Another method that overcomes the limitations of classical electroless deposition is substrate-enhanced electroless deposition (SEED). In the SEED method, CNTs are supported with metal substrates whose redox potential is suitably lower than that of the metal species being reduced. In this case, CNTs are no longer a reducing agent and act only as cathodes and templates for metal deposition from the corresponding noble-metal salts [214].

4.1.3. Noble-Metal Nanoparticles on Graphene

In addition to carbon nanotubes, graphene (GR) as carbon support also improves the catalytic activity and stability of supported Pt catalysts compared to mesoporous counterparts through enhanced electrical conductivity and metal–substrate interaction [181]. Graphene is a single-atom-thick two-dimensional carbon nanosheet of sp^2 bonded carbon atoms packed into a honeycomb lattice that was first synthesized in 2004 by Geim and Novoselov [272]. In 2010, this discovery was awarded the Nobel Prize in Physics for its significant contributions to the development of graphene-based catalysts [273]. Over the years, graphene, as well as its derivatives, including graphene oxide (GO) and reduced graphene oxide (rGO), have become promising candidates for many applications such as batteries, photovoltaic devices, biosensors, supercapacitors and fuel cells. This wide range of applicability is influenced by its unique properties such as large surface area, thermal conductivity, high electron mobility and good stability [159,177,274,275]. Significantly, the numerous oxygen-containing groups present in GO and rGO provide many opportunities for further functionalization and modification [276–279]. Graphene is an excellent building block in the fabrication of various nanocomposites representing the most recent advance in many fields of chemistry, physics, and electronics [219,274,275,280,281]. Combining GR with noble-metal nanoparticles improves electrochemical performance and provides perfect thermal stability, which is important in electrocatalytic applications (e.g., oxygen reduction and hydrogen/oxygen evolution reactions) [282,283].

The preparation of GR-based noble-metal nanocomposites by using wet-chemical synthesis methods has many advantages, such as an economic cost of production, high yield, mass production and commonness. The most popular strategy is the direct chemical reduction of a noble metal precursor (e.g., $HAuCl_4$, $AgNO_3$, H_2PdCl_4 or K_2PtCl_4) in the presence of graphene and its derivative sheets using a reducing agent such as amines, $NaBH_4$, and ascorbic acid [284–286]. For example, Iqbal's group prepared 34 nm mesoporous Pd nanoparticles on rGO sheets modified by the block copolymer F127 [287]. This block copolymer has served as a template for better dispersion of Pd nanoparticles. As a precursor to palladium particles, H_2PdCl_4 was used , which was reduced by ascorbic acid. By using direct chemical reduction, it is also possible to synthesize GR-based multimetallic noble-metal nanocomposites. For example, Pt-Pd supported on rGO were obtained by the reduction of a noble-metal precursor (H_2PtCl_6 and $PdCl_2$) by ascorbic acid and octylphenoxypolyethoxyethanol (NP-40) as a soft template [288]. Vilian et al. reported the synthesis of Pt-Au/rGO nanohybrids by a direct chemical-reduction methodology. The reported methanol oxidation is found to exhibit excellent electrocatalytic performance, reliability, and stability, surpassing that of several reported modified electrodes that can also be used for platinum-based catalysts in fuel-cell applications [289].

The chemical reduction process can also be assisted by microwave irradiation for the synthesis of chemically converted graphene sheets and metal nanoparticles dispersed on them [290]. In turn, the sonochemical method has been used, for example, in the development of Au/GR nanocomposite [291]. In this study, by using an ultrasonication probe of 20 kHz on the surface of exfoliated few-layer graphene sheets, the in situ growth of gold nanoparticles (Au NPs) after the reduction of gold chloride took place . Alternatively, Huang et al. synthesized Pd/rGO nanohybrids with ~3 nm nanoparticles using a one-pot photoassisted citrate reduction. In the process shown, the mixture of GO solution, Na_2PdCl_4, sodium citrate, and deionized water was irradiated by a 500 W high-pressure mercury lamp for 12 h. This synthetic approach allows for the formation onto the rGO surface of Pd nanoparticles with the desired size with excellent activity and stability of complexes in oxygen reduction and ethanol oxidation reactions. The prepared Pd/rGO nanocomposite exhibited 5.2 times higher mass activity for ethanol oxidation reaction than the commercial Pt/C catalyst [292].

By analogy with other carbonaceous supports, it is possible to use an electroless method to prepare NMNPs/GR composites. In this case, graphene derivatives (GO or rGO) themselves can donate electrons to reduce the noble-metal precursors in an aqueous phase without any additional reductant. In accordance with this, metal precursors (e.g., $HAuCl_4$, H_2PdCl_4, or $AgNO_3$) can be reduced to form metallic Au, Pd, and Ag nanoparticles, respectively, solely by GO or rGO [284,293,294]. An example would be the work of [295], in the synthesis of the redox reaction between Au, Ag or Pd precursors and the partially reduced graphene oxide (prGO) in an aqueous solution. The as-obtained Au, Ag and Pd/prGO nanocomposites display excellent catalytic activities, and the size distributions of the Au, Ag, and Pd particles were 1–20 nm, 3–10 nm and 0.5–3 nm, respectively.

Interesting conclusions presented by Qin et al. claim that a heating treatment and strong alkaline conditions enhance the reducing ability of the hydroxyl groups on GO. In their work, Au/rGO nanocomposites were prepared through a one-pot strategy, conducted by heating a mixture of $HAuCl_4$, NaOH and graphene oxide solution at 90 °C [294]. It is also possible to obtain NMNPs/GR nanocomposites by using pure graphene without any additional groups. This strategy was proposed in a paper by Jeong et al., in which graphene was covered onto a reducing substrate (e.g., Si or Al) [286]. As a result, Au/GR or Pt/GR nanocomposites could be prepared because electrons were transferred from the substrate, via graphene, to the precursors ($HAuCl_4$ or $KPtCl_4$). In Zou et al.'s paper, using a two-step electrochemical deposition method, spherical Au nanoparticles and a 3D flower-like structure graphene were obtained on a glassy carbon electrode (Au/rGE/GCE) [296]. Another example was presented by Liu et al.: an electrochemically seed-mediated method by which sub-10 nm tetrahexahedral (THH) Pt NCs supported on graphene were synthesized. The

obtained nanohybrids exhibited a higher mass activity than a commercial Pt/C catalyst for ethanol electrooxidation [297].

All of the GR-based nanohybrid examples presented above focus on graphene and its derivatives' 2D morphology. However, the practical application of graphene is associated with difficulties in the form of the stacking and folding of its sheets. In particular, it is hindered by 2D GR wrinkles that wrap around MNNPs. This limits electron and mass transport and makes its application in electrocatalysis much more difficult [298]. Therefore, the focus has been on designing various 3D GR nanostructures (e.g., framework, network, foam, etc.). These treatments aim to minimize wrinkles as well as reduce agglomeration of nanoparticles [299–302]. Qiu et al., by using a layer-by-layer assembly method, presented a versatile synthesis strategy based on sacrificial templates to obtain three-dimensional graphene-assisted PtM (M = Fe, Co, Ni) nanospheres [303]. In the first step, electrostatic attraction was used to wind 2D GO sheets on positively charged SiO2 nanospheres. Next, PtM (M = Fe, Co, Ni) alloy nanoparticles were deposited on the surface of 3D rGO nanospheres. Finally, after etching SiO_2, the 3D rGO-supported PtM hollow nanospheres were formed. These nanocomposites exhibit enhanced electrocatalytic activity, durability, and stability for methanol oxidation reactions (MOR), compared with commercial Pt/C. On the other hand, Yao et al. showed that Pd nanoparticles encapsulated in hollow microspheres of N-doped graphene, exhibited higher EOR activity in an alkaline medium than Pd/rGO [304]. Additionally, it should be noted that the structure of N-doped GR hollow microspheres greatly facilitates the diffusion of reactants, which, in turn, improves the catalytic reactions [305].

Reducing the particle size of noble metals positively affects the activity of the catalysts constructed on their basis, by significantly increasing the specific activity per metal atom. Therefore, single-atom catalysts (SACs) containing single-metal atoms anchored on supports are sought. The surface of pristine graphene and metal atoms are not firmly fixed, and they easily diffuse together to form nanoparticles [306]. Therefore, obtaining dispersed metal atoms on pure GR is difficult. Accordingly, the surfaces of an ultrathin thickness and large specific surface area of 2D GR nanosheets have been doped with heteroatoms such as N, O, or S, which provide anchors for SAC (Figure 8) [307].

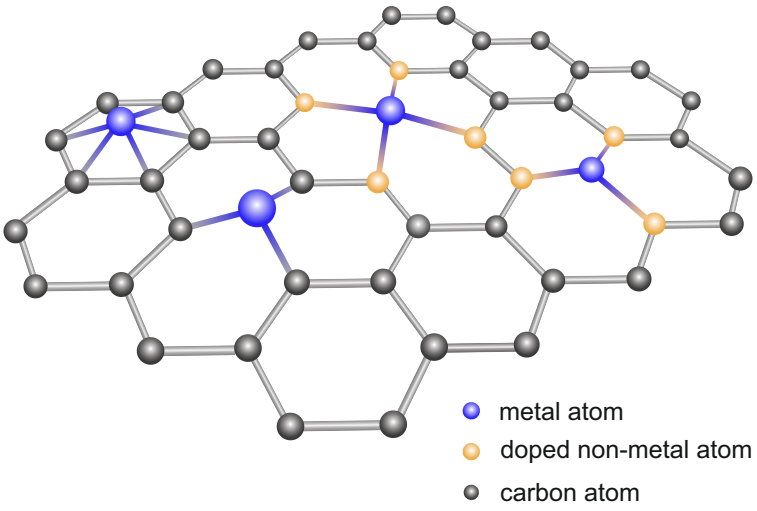

Figure 8. Scheme of doped graphene nanosheets with single-atom catalysts.

The atomic layer deposition (ALD) technique has become a promising method to obtain monoatomic catalysts on graphene derivatives [306,308,309]. This cyclic process was based on sequential self-terminating reactions between a solid surface and gas-phase precursor molecules [310]. For example, Sun et al. described the practical construction of isolated Pt atoms anchored in graphene nanosheets (GNSs) using the ALD method [311]. In the construction process, oxygen and (methylcyclopentadienyl)-trimethyl platinum ($MeCpPtMe_3$) were used as precursors. In the first step, the number of oxygen-functional

groups on the rGO surface was selected to form a thin Pt monolayer. Subsequently, oxygen exposure formed new surface oxygen on the pre-existing Pt layer. This process completed one cycle of a complete reaction. The morphology, size and loading density of platinum over graphene were controlled by simply tuning the cycles of the ALD (i.e., 50, 100, and 150 cycles). Finally, the best results, i.e., single Pt atoms, were obtained after 50 ALD cycles. All the discussed ALDPt/GNSs catalysts show several-times-higher activity for MOR than the Pt/C catalyst. Among them, ALD50Pt/GNS is more than 9.5 times more active than the Pt/C catalyst. Another example of using the ALD method was presented by Yan et al. They described the growth of single Pd atoms anchored to phenyl groups on rGO substrates [309]. Using the same method, they also presented the deposition of Pt_2 dimers on graphene [312].

Wet impregnation is another method for the synthesis of single noble-metal atoms supported on graphene [313–315]. For example, Zhang et al. synthesized single Ru atoms on N-doped GD [314]. For example, Zhang et al. synthesized single Ru atoms on N-doped GO by using the $Ru(NH_3)_6Cl_3$ as a precursor. The mixture thus formed was lyophilized to prevent the restacking of GO sheets. The resulting GO impregnated with Ru atoms was annealed in NH_3 gas at 750 °C. This process led to the reduction of GO to form GR. Finally, nitrogen atoms were doped into the graphene plane as anchor sites for ruthenium atoms.

5. Conclusions

The history of noble-metal nanoparticles presented in this article dates back to the antiquity and extends to recent years, in which thousands of scientists, still, have been looking for the perfect nanoparticle. This research has been carried out by examining their various shapes, sizes, and elemental compositions, including the possibility of combining them with carbon substrates allowing for the enhancement of the expected and so much desired catalytic properties.

The research concerning carbon-supported NMNPs and their electrocatalytic activity has been rapidly developing in the previous years. Various forms of carbon, such as MCs, CNTs, fullerenes, GRs, etc., have been successfully used as promising substrate candidates for noble-metal nanoparticles for fuel-cell catalysts. Until now, much effort has gone into low-cost, simple, and controlled methods for producing NMNPs/carbon hybrids in order to obtain a specific surface area and uniform nanoparticle dispersions. Special attention is given to the fact that reducing the Pt loading can decrease the fuel-cell cost, while the suitable supporting materials can enhance the long-term durability and thus can achieve excellent catalytic performance. Moreover, numerous reports indicate that the use of multimetallic electrocatalysts can improve performance stability.

Among the vast literature on carbon-supported nanoparticles, there is no universal type that would be suitable for all applications. Every year, many papers are published showing more and more perfect solutions for specific applications. However, there are still no catalysts efficient enough to fully meet the needs of fuel-cell manufacturers and enable the commercialization of such devices.

The development of high-performance and inexpensive catalysts based on metallic nanoparticles would allow the widespread commercialization of hydrogen technology. However, bearing in mind the growing demand for energy, if only because of the ever-increasing population of our globe, this technology is essential for the further development of humanity. Introducing it into common use would allow the implementation of many climate-protection procedures without the need to introduce major changes in human behavior, because hydrogen technology allows almost unlimited access to renewable energy sources in an ecological and emission-free manner.

Author Contributions: Conceptualization: M.L., A.K.; data curation: M.L., A.K.; funding acquisition: M.L., A.K.; project administration: M.L., A.K.; resources: M.L., A.K.; software: M.L., M.A.; supervision: M.L., P.K.; validation: P.K., M.A., S.E.H.; visualization: M.L.; writing—original draft: M.L., A.K., P.K., M.A., S.E.H.; writing—review and editing: M.L., A.K. All authors have read and agreed to the published version of the manuscript.

Funding: This work was supported by the resources of the National Science Centre (Grant-No: 2021/05/X/ST5/01296)

Institutional Review Board Statement: Not applicable.

Informed Consent Statement: Not applicable.

Data Availability Statement: Not applicable.

Conflicts of Interest: The authors declare no conflict of interest.

Abbreviations

The following abbreviations are used in this manuscript:

AA	Ascorbic Acid
AFC	Alkaline Fuel Cells
ALD	Atomic Layer Deposition
BDD	Boron-Doped Diamond
C	Carbon
CA	Carbon Aerogel
CB	Carbon Black
CCA	Citric Acid
CM	Carbonaceous Material
CNF	Carbon Nanofiber
CNO	Carbon Nanoonion
CNT	Carbon Nanotube
CP	Carbon paper
CTAB	Cetyltrimethylammonium Bromide
CQD	Carbon Quantum Dot
CX	Carbon Xerogels
DEFC	Direct Ethanol Fuel Cell
DEG	Diethylene Glycol
DMFC	Direct Methanol Fuel Cell
EG	Ethylene Glycol
EOR	Ethanol Oxidation Reaction
G	Graphene
GCE	Glassy Carbon Electrode
GMC	Graphitic Mesoporous Carbon
GNS	Graphene Nanosheet
GO	Graphene Oxide
HA	Hydroxylamine
HEA	High-Entropy Alloy
HEPES	4-(2-hydroxyethyl)-1- piperazineethanesulfonic Acid
HER	Hydrogen Evolution Reaction
HOR	Hydrogen Oxidation Reaction
MCFC	Molten Carbonate Fuel Cells
MEA	Membrane-Electrode Assembly
MeCpPtMe3	Methylcyclopentadienyl)-trimethyl platinum
MNC	Marimo Nanocarbon
MOR	Methanol Oxidation Reaction
MWCNT	Multiwalled Carbon Nanotube
N-GN	Nitrogen-doped Graphite Nanosheet
NMNP	Noble Metal Nanoparticle
NP	Nanoparticle
NW	Nanowire
NYPA	Naphthalen-1-ylmethylphosphonic Acid
ORR	Oxygen Reduction Reaction
PC	Porous Carbon

PCN	Porous Carbon Nanosphere
PDDA	poly(diallyldimethyl ammonium) chloride
PEG	Polyethylene Glycol
PEI	Polyethyleneimine
PEMFC	Proton-Exchange Membrane Fuel Cell
POLE	Polyoxyethylene Lauryl Ether
prGO	Partially Reduced Graphene Oxide
PSD	Potentiostatic Deposition
PSWD	Potential Square Wave Deposition
PVA	Polyvinyl Alcohol
PVP	Polyvinyl Pyrrolidone
PyrC60	Fullerene-pyrolidine
RFC	Regenerative Fuel Cells
rGO	Reduced Graphene Oxide
SA	Sodium Ascorbate
SAC	Single-Atom Catalyst
SC	Sodium Citrate
SDBS	Sodium Dodecyl Benzene Sulfonate
SDS	Sodium Dodecyl Sulfate
SEED	Substrate Enhanced Electroless Deposition
SOFC	Solid-Oxide Fuel Cells
SWCNT	Single-Walled Carbon Nanotube
TA	Tannic Acid
TEG	Tetraethylene Glycol
THF	tetrahydrofuran
TREG	Triethylene Glycol
URFC	Unitized Regenerative Fuel Cells

References

1. Habashi, F. Gold–An historical introduction. In *Gold Ore Processing*; Elsevier: Amsterdam, The Netherlands, 2016; pp. 1–20.
2. Vajtai, R. *Springer Handbook of Nanomaterials*; Springer Science & Business Media: New York, NY, USA, 2013.
3. Louis, C.; Pluchery, O. *Gold Nanoparticles for Physics, Chemistry and Biology*; World Scientific: Singapore, 2017.
4. Ebrahiminezhad, A.; Raee, M.J.; Manafi, Z.; Sotoodeh Jahromi, A.; Ghasemi, Y. Ancient and novel forms of silver in medicine and biomedicine. *J. Adv. Med Sci. Appl. Technol.* **2016**, *2*, 122–128.
5. Mingos, D.M.P.; Broda, J. *Gold Clusters, Colloids and Nanoparticles I*; Springer: Berlin/Heidelberg, Germany, 2014; Volume 161.
6. Tweney, R.D. Discovering discovery: How Faraday found the first metallic colloid. *Perspect. Sci.* **2006**, *14*, 97–121.
7. Faraday, M. X. The Bakerian Lecture.—Experimental relations of gold (and other metals) to light. *Philos. Trans. R. Soc. Lond.* **1857**, *147*, 145–181.
8. Wu, D.; Kusada, K.; Yamamoto, T.; Toriyama, T.; Matsumura, S.; Kawaguchi, S.; Kubota, Y.; Kitagawa, H. Platinum-group-metal high-entropy-alloy nanoparticles. *J. Am. Chem. Soc.* **2020**, *142*, 13833–13838.
9. Astruc, D. Introduction: Nanoparticles in Catalysis. *Chem. Rev.*, **2020**, *120*, 461–463.
10. Haruta, M.; Kobayashi, T.; Sano, H.; Yamada, N. Novel gold catalysts for the oxidation of carbon monoxide at a temperature far below 0 C. *Chem. Lett.* **1987**, *16*, 405–408.
11. Brenan, J.M. The platinum-group elements: "Admirably adapted" for science and industry. *Elements* **2008**, *4*, 227–232.
12. Wu, D.; Kusada, K.; Nanba, Y.; Koyama, M.; Yamamoto, T.; Toriyama, T.; Matsumura, S.; Seo, O.; Gueye, I.; Kim, J.; et al. Noble-Metal High-Entropy-Alloy Nanoparticles: Atomic-Level Insight into the Electronic Structure. *J. Am. Chem. Soc.* **2022**, *144*, 3365–3369.
13. Wang, Y.; Leung, D.Y.; Xuan, J.; Wang, H. A review on unitized regenerative fuel cell technologies, part B: Unitized regenerative alkaline fuel cell, solid oxide fuel cell, and microfluidic fuel cell. *Renew. Sustain. Energy Rev.* **2017**, *75*, 775–795.
14. Kee, R.J.; Zhu, H.; Goodwin, D.G. Solid-oxide fuel cells with hydrocarbon fuels. *Proc. Combust. Inst.* **2005**, *30*, 2379–2404.
15. Cropper, M.A.; Geiger, S.; Jollie, D.M. Fuel cells: A survey of current developments. *J. Power Sources* **2004**, *131*, 57–61.
16. Antolini, E.; Salgado, J.; Santos, L.; Garcia, G.; Ticianelli, E.; Pastor, E.; Gonzalez, E. Carbon supported Pt–Cr alloys as oxygen-reduction catalysts for direct methanol fuel cells. *J. Appl. Electrochem.* **2006**, *36*, 355–362. doi:10.1007/s10800-005-9072-0.
17. Li, L.; Wu, G.; Ye, Q.; Deng, W.; Xu, B. RESEARCH PAPER. *Acta-Phys.-Chim. Sin.* **2006**, *22*, 419–423. doi:10.1016/S1872-1508(06)60013-2.
18. Ralph, T.; Hards, G.; Keating, J.; Campbell, S.; Wilkinson, D.; Davis, M.; St-Pierre, J.; Johnson, M. ChemInform Abstract: Low Cost Electrodes for Proton Exchange Membrane Fuel Cells. Performance in Single Cells and Ballard Stacks. *J. Electrochem. Soc.* **1997**, *144*, 3845–3857.

19. Panayiotou, G.P.; Kalogirou, S.A.; Tassou, S.A. PEM fuel cells for energy production in solar hydrogen systems. *Recent Patents Mech. Eng.* **2010**, *3*, 226–235.
20. Katz, E. Electrochemical contributions: William Nicholson (1753–1815). *Electrochem. Sci. Adv.* **2021**, *1*, e2160003. doi:10.1002/elsa.202160003.
21. Andújar, J.M.; Segura, F. Fuel cells: History and updating. A walk along two centuries. *Renew. Sustain. Energy Rev.* **2009**, *13*, 2309–2322.
22. Scholz, F. Wilhelm Ostwald's role in the genesis and evolution of the Nernst equation. *J. Solid State Electrochem.* **2017**, *21*, 1847–1859.
23. Fan, L.; Tu, Z.; Chan, S.H. Recent development of hydrogen and fuel cell technologies: A review. *Energy Rep.* **2021**, *7*, 8421–8446.
24. Choudhury, S.; Acharya, S.K.; Khadanga, R.K.; Mohanty, S.; Arshad, J.; Ur Rehman, A.; Shafiq, M.; Choi, J.G. Harmonic Profile Enhancement of Grid Connected Fuel Cell through Cascaded H-Bridge Multi-Level Inverter and Improved Squirrel Search Optimization Technique. *Energies* **2021**, *14*, 7947.
25. Zhao, F.; Zheng, L.; Yuan, Q.; Yang, X.; Zhang, Q.; Xu, H.; Guo, Y.; Yang, S.; Zhou, Z.; Gu, L.; et al. Ultrathin PdAuBiTe Nanosheets as High-Performance Oxygen Reduction Catalysts for a Direct Methanol Fuel Cell Device. *Adv. Mater.* **2021**, *33*, 2103383.
26. Xiao, F.; Wang, Y.C.; Wu, Z.P.; Chen, G.; Yang, F.; Zhu, S.; Siddharth, K.; Kong, Z.; Lu, A.; Li, J.C.; et al. Recent advances in electrocatalysts for proton exchange membrane fuel cells and alkaline membrane fuel cells. *Adv. Mater.* **2021**, *33*, 2006292.
27. Zhang, S.; Shao, Y.; Yin, G.; Lin, Y. Recent progress in nanostructured electrocatalysts for PEM fuel cells. *J. Mater. Chem. A* **2013**, *1*, 4631–4641.
28. Haile, S.M. Fuel cell materials and components. *Acta Mater.* **2003**, *51*, 5981–6000.
29. Knights, S.D.; Colbow, K.M.; St-Pierre, J.; Wilkinson, D.P. Aging mechanisms and lifetime of PEFC and DMFC. *J. Power Sources* **2004**, *127*, 127–134. doi:10.1016/j.jpowsour.2003.09.033.
30. Schultz, T.; Zhou, S.; Sundmacher, K. Current status of and recent developments in the direct methanol fuel cell. *Chem. Eng. Technol.* **2001**, *24*, 1223–1233.
31. Gouda, M.; Elnouby, M.; Aziz, A.N.; Youssef, M.E.; Santos, D.; Elessawy, N.A. Green and low-cost membrane electrode assembly for proton exchange membrane fuel cells: Effect of double-layer electrodes and gas diffusion layer. *Front. Mater.* **2020**, *6*, 337.
32. Peighambardoust, S.J.; Rowshanzamir, S.; Amjadi, M. Review of the proton exchange membranes for fuel cell applications. *Int. J. Hydrogen Energy* **2010**, *35*, 9349–9384.
33. Beermann, V.; Holtz, M.E.; Padgett, E.; de Araujo, J.F.; Muller, D.A.; Strasser, P. Real-time imaging of activation and degradation of carbon supported octahedral Pt–Ni alloy fuel cell catalysts at the nanoscale using in situ electrochemical liquid cell STEM. *Energy Environ. Sci.* **2019**, *12*, 2476–2485.
34. Li, S.; Tang, X.; Jia, H.; Li, H.; Xie, G.; Liu, X.; Lin, X.; Qiu, H.J. Nanoporous high-entropy alloys with low Pt loadings for high-performance electrochemical oxygen reduction. *J. Catal.* **2020**, *383*, 164–171.
35. Yu, K.; Groom, D.J.; Wang, X.; Yang, Z.; Gummalla, M.; Ball, S.C.; Myers, D.J.; Ferreira, P.J. Degradation mechanisms of platinum nanoparticle catalysts in proton exchange membrane fuel cells: The role of particle size. *Chem. Mater.* **2014**, *26*, 5540–5548.
36. Jayabal, S.; Saranya, G.; Geng, D.; Lin, L.Y.; Meng, X. Insight into the correlation of Pt–support interactions with electrocatalytic activity and durability in fuel cells. *J. Mater. Chem. A* **2020**, *8*, 9420–9446.
37. Grigoriev, S.; Millet, P.; Fateev, V. Evaluation of carbon-supported Pt and Pd nanoparticles for the hydrogen evolution reaction in PEM water electrolysers. *J. Power Sources* **2008**, *177*, 281–285.
38. Edwards, P.; Thomas, J. Gold in a Metallic Divided Stateâ€"From Faraday to Present-Day Nanoscience. *Angew. Chem. Int. Ed.* **2007**, *46*, 5480–5486.
39. Pareek, V.; Bhargava, A.; Gupta, R.; Jain, N.; Panwar, J. Synthesis and Applications of Noble Metal Nanoparticles: A Review. *Adv. Sci. Eng. Med.* **2017**, *9*, 527–544.
40. De Oliveira, P.F.M.; Torresi, R.M.; Emmerling, F.; Camargo, P.H.C. Challenges and opportunities in the bottom-up mechanochemical synthesis of noble metal nanoparticles. *J. Mater. Chem. A* **2020**, *8*, 16114–16141. doi:10.1039/D0TA05183G.
41. Booth, S.G.; Uehara, A.; Chang, S.Y.; Mosselmans, J.F.W.; Schroeder, S.L.M.; Dryfe, R.A.W. Gold Deposition at a Free-Standing Liquid/Liquid Interface: Evidence for the Formation of Au(I) by Microfocus X-ray Spectroscopy (μXRF and μXAFS) and Cyclic Voltammetry. *J. Phys. Chem. C* **2015**, *119*, 16785–16792. doi:10.1021/acs.jpcc.5b05127.
42. Starowicz, M.; Stypuła, B. Electrochemical Synthesis of ZnO Nanoparticles. *Eur. J. Inorg. Chem.* **2008**, *2008*, 869–872. doi:10.1002/ejic.200700989.
43. Balachandramohan, J.; Sivasankar, T.; Sivakumar, M. Facile sonochemical synthesis of Ag2O-guar gum nanocomposite as a visible light photocatalyst for the organic transformation reactions. *J. Hazard. Mater.* **2020**, *385*, 121621. doi:10.1016/j.jhazmat.2019.121621.
44. Noman, M.T.; Petru, M.; Militký, J.; Azeem, M.; Ashraf, M.A. One-Pot Sonochemical Synthesis of ZnO Nanoparticles for Photocatalytic Applications, Modelling and Optimization. *Materials* **2020**, *13*, 14. doi:10.3390/ma13010014.
45. Sharma, D.; Kanchi, S.; Bisetty, K. Biogenic synthesis of nanoparticles: A review. *Arab. J. Chem.* **2019**, *12*, 3576–3600. doi:10.1016/j.arabjc.2015.11.002.
46. Ahmad, S.; Munir, S.; Zeb, N.; Ullah, A.; Khan, B.; Ali, J.; Bilal, M.; Omer, M.; Alamzeb, M.; Salman, S.M.; et al. Green nanotechnology: A review on green synthesis of silver nanoparticles—An ecofriendly approach. *Int. J. Nanomed.* **2019**, *14*, 5087.
47. Jain, K. Nanomedicine: Application of Nanobiotechnology in Medical Practice. *Med Princ. Pract.* **2008**, *17*, 89–101. doi:10.1159/000112961.

48. Košević, M.G.; Zarić, M.M.; Stopić, S.R.; Stevanović, J.S.; Weirich, T.E.; Friedrich, B.G.; Panić, V.V. Structural and Electrochemical Properties of Nesting and Core/Shell Pt/TiO_2 Spherical Particles Synthesized by Ultrasonic Spray Pyrolysis. *Metals* **2020**, *10*, 11. doi:10.3390/met10010011.
49. Lusker, K.L.; Li, J.R.; Garno, J.C. Nanostructures of Functionalized Gold Nanoparticles Prepared by Particle Lithography with Organosilanes. *Langmuir* **2011**, *27*, 13269–13275. doi:10.1021/la202816k.
50. Yu, X.; Pham, J.T.; Subramani, C.; Creran, B.; Yeh, Y.C.; Du, K.; Patra, D.; Miranda, O.R.; Crosby, A.J.; Rotello, V.M. Direct Patterning of Engineered Ionic Gold Nanoparticles via Nanoimprint Lithography. *Adv. Mater.* **2012**, *24*, 6330–6334. doi:10.1002/adma.201202776.
51. Davies, G.L.; O'Brien, J.; Gun'ko, Y.K. Rare Earth Doped Silica Nanoparticles via Thermolysis of a Single Source Metallasilsesquioxane Precursor. *Sci. Rep.* **2017**, *7*, 45862. doi:10.1038/srep45862.
52. Abedini, A.; Daud, A.R.; Abdul Hamid, M.A.; Kamil Othman, N.; Saion, E. A review on radiation-induced nucleation and growth of colloidal metallic nanoparticles. *Nanoscale Res. Lett.* **2013**, *8*, 474. doi:10.1186/1556-276X-8-474.
53. Mirzaei, A.; Neri, G. Microwave-assisted synthesis of metal oxide nanostructures for gas sensing application: A review. *Sensors Actuators B Chem.* **2016**, *237*, 749–775. doi:10.1016/j.snb.2016.06.114.
54. Habibullah, G.; Viktorova, J.; Ruml, T. Current Strategies for Noble Metal Nanoparticle Synthesis. *Nanoscale Res. Lett.* **2021**, *16*, 47.
55. Herizchi, R.; Abbasi, E.; Milani, M.; Akbarzadeh, A. Current methods for synthesis of gold nanoparticles. *Artif. Cells Nanomed. Biotechnol.* **2016**, *44*, 596–602.
56. Reverberi, A.; Kuznetsov, N.; Meshalkin, V.; Salerno, M.; Fabiano, B. Systematical analysis of chemical methods in metal nanoparticles synthesis. *Theor. Found. Chem. Eng.* **2016**, *50*, 59–66.
57. Silva, L.I.; Perez-Gramatges, A.; Larrude, D.G.; Almeida, J.M.; Aucélio, R.Q.; da Silva, A.R. Gold nanoparticles produced using NaBH4 in absence and in the presence of one-tail or two-tail cationic surfactants: Characteristics and optical responses induced by aminoglycosides. *Colloids Surfaces Physicochem. Eng. Asp.* **2021**, *614*, 126174.
58. Moonrat, C.; Kittinaovarut, S.; Jinawath, S.; Sujaridworakun, P. The Effect of pH Values on Color Development of Silver Colloids. In *Key Engineering Materials*; Trans Tech Publications Ltd.: Freienbach, Switzerland, 2020; Volume 862, pp. 17–21.
59. Mehr, F.P.; Khanjani, M.; Vatani, P. Synthesis of nano-Ag particles using sodium borohydride. *Orient. J. Chem.* **2015**, *31*, 1831–1833.
60. Sudirman, S.; Adi, W.A.; Budianto, E.; Yudianti, R. Mono-Dispersed Pt/MWNTs: Growing Directly on Multiwall Carbon Nanotubes (MWNTs) Using NaBH4 as Reducing Agent for Component of Proton Exchange Membrane Fuel Cell (PEMFC). *Int. J. Chem.* **2020**, *12*, 37–48.
61. Jung, S.C.; Park, Y.K.; Jung, H.Y.; Kim, S.C. Effect of Stabilizing Agents on the Synthesis of Palladium Nanoparticles. *J. Nanosci. Nanotechnol.* **2017**, *17*, 2833–2836.
62. Günbatar, S.; Aygun, A.; Karataş, Y.; Gülcan, M.; Şen, F. Carbon-nanotube-based rhodium nanoparticles as highly-active catalyst for hydrolytic dehydrogenation of dimethylamineborane at room temperature. *J. Colloid Interface Sci.* **2018**, *530*, 321–327.
63. Patharkar, R.; Nandanwar, S.; Chakraborty, M. Synthesis of colloidal ruthenium nanocatalyst by chemical reduction method. *J. Chem.* **2013**, *2013*, 831694.
64. He, S.B.; Zhuang, Q.Q.; Yang, L.; Lin, M.Y.; Kuang, Y.; Peng, H.P.; Deng, H.H.; Xia, X.H.; Chen, W. A Heparinase Sensor Based on a Ternary System of Hg^{2+}–Heparin–Osmium Nanoparticles. *Anal. Chem.* **2019**, *92*, 1635–1642.
65. Cui, M.; Huang, X.; Zhang, X.; Xie, Q.; Yang, D. Ultra-small iridium nanoparticles as active catalysts for the selective and efficient reduction of nitroarenes. *New J. Chem.* **2020**, *44*, 18274–18280.
66. Ahmadi, T.S.; Wang, Z.L.; Green, T.C.; Henglein, A.; El-Sayed, M.A. Shape-Controlled Synthesis of Colloidal Platinum Nanoparticles. *Science* **1996**, *272*, 1924–1925. doi:10.1126/science.272.5270.1924.
67. Petroski, J.M.; Wang, Z.L.; Green, T.C.; El-Sayed, M.A. Kinetically Controlled Growth and Shape Formation Mechanism of Platinum Nanoparticles. *J. Phys. Chem. B* **1998**, *102*, 3316–3320. doi:10.1021/jp981030f.
68. Yu, Y.T.; Xu, B.Q. Shape-controlled synthesis of Pt nanocrystals: An evolution of the tetrahedral shape. *Appl. Organomet. Chem.* **2006**, *20*, 638–647. doi:10.1002/aoc.1123.
69. Sau, T.K.; Murphy, C.J. Role of ions in the colloidal synthesis of gold nanowires. *Philos. Mag.* **2007**, *87*, 2143–2158. doi:10.1080/14786430601110356.
70. Sun, Y.; Zhang, L.; Zhou, H.; Zhu, Y.; Sutter, E.; Ji, Y.; Rafailovich, M.H.; Sokolov, J.C. Seedless and Templateless Synthesis of Rectangular Palladium Nanoparticles. *Chem. Mater.* **2007**, *19*, 2065–2070. doi:10.1021/cm0623209.
71. Kuwahara, Y.; Yoshimori, K.; Tomita, K.; Sakai, M.; Sawada, T.; Niidome, Y.; Yamada, S.; Shosenji, H. Novel effects of twin-tailed cationic surfactants on the formation of gold nanorods. *Chem. Lett.* **2007**, *36*, 1230–1231. doi:10.1246/cl.2007.1230.
72. Sui, Z.; Chen, X.; Wang, L.; Xu, L.; Zhuang, W.; Chai, Y.; Yang, C. Capping effect of CTAB on positively charged Ag nanoparticles. *Phys. E Low-Dimens. Syst. Nanostructures* **2006**, *33*, 308–314. doi:10.1016/j.physe.2006.03.151.
73. Skrabalak, S.E.; Au, L.; Li, X.; Xia, Y. Facile synthesis of Ag nanocubes and Au nanocages. *Nat. Protoc.* **2007**, *2*, 2182–2190. doi:10.1038/nprot.2007.326.
74. Rogach, A.L.; Shevchenko, G.P.; Afanas'ev, Z.M.; Sviridov, V.V. Changes in the Morphology and Optical Absorption of Colloidal Silver Reduced with Formic Acid in the Polymer Matrix under UV Irradiation. *J. Phys. Chem. B* **1997**, *101*, 8129–8132. doi:10.1021/jp971350j.
75. Kou, X.; Zhang, S.; Yang, Z.; Tsung, C.K.; Stucky, G.D.; Sun, L.; Wang, J.; Yan, C. Glutathione- and Cysteine-Induced Transverse Overgrowth on Gold Nanorods. *J. Am. Chem. Soc.* **2007**, *129*, 6402–6404. doi:10.1021/ja0710508.

76. Bakshi, M.S.; Sachar, S.; Kaur, G.; Bhandari, P.; Kaur, G.; Biesinger, M.C.; Possmayer, F.; Petersen, N.O. Dependence of crystal growth of gold nanoparticles on the capping behavior of surfactant at ambient conditions. *Cryst. Growth Des.* **2008**, *8*, 1713–1719. doi:10.1021/cg8000043.
77. Wang, Z.L. Transmission Electron Microscopy of Shape-Controlled Nanocrystals and Their Assemblies. *J. Phys. Chem. B* **2000**, *104*, 1153–1175. doi:10.1021/jp993593c.
78. Arán Ais, R.M.; Vidal-Iglesias, F.; Solla-Gullon, J.; Herrero, E.; Feliu, J. Electrochemical Characterization of Clean Shape-Controlled Pt Nanoparticles Prepared in Presence of Oleylamine/Oleic Acid. *Electroanalysis* **2015**, *27*, 945–956. doi:10.1002/elan.201400619.
79. Montiel, M.; Vidal-Iglesias, F.; Montiel, V.; Solla-Gullón, J. Electrocatalysis on shape-controlled metal nanoparticles: Progress in surface cleaning methodologies. *Curr. Opin. Electrochem.* **2017**, *1*, 34–39. doi:10.1016/j.coelec.2016.12.007.
80. Niu, W.; Zhang, L.; Xu, G. Seed-mediated growth of noble metal nanocrystals: Crystal growth and shape control. *Nanoscale* **2013**, *5*, 3172–3181. doi:10.1039/C3NR00219E.
81. Nikoobakht, B.; El-Sayed, M.A. Preparation and growth mechanism of gold nanorods (NRs) using seed-mediated growth method. *Chem. Mater.* **2003**, *15*, 1957–1962.
82. Ward, C.J.; Tronndorf, R.; Eustes, A.S.; Auad, M.L.; Davis, E.W. Seed-mediated growth of gold nanorods: Limits of length to diameter ratio control. *J. Nanomater.* **2014**, *2014*.
83. Mondal, J.; Trinh, Q.T.; Jana, A.; Ng, W.K.H.; Borah, P.; Hirao, H.; Zhao, Y. Size-Dependent Catalytic Activity of Palladium Nanoparticles Fabricated in Porous Organic Polymers for Alkene Hydrogenation at Room Temperature. *ACS Appl. Mater. Interfaces* **2016**, *8*, 15307–15319. doi:10.1021/acsami.6b03127.
84. Li, M.; Zhao, Z.; Cheng, T.; Fortunelli, A.; Chen, C.Y.; Yu, R.; Zhang, Q.; Gu, L.; Merinov, B.V.; Lin, Z.; et al. Ultrafine jagged platinum nanowires enable ultrahigh mass activity for the oxygen reduction reaction. *Science* **2016**, *354*, 1414–1419. doi:10.1126/science.aaf9050.
85. Wang, H.; Chen, H.; Ni, B.; Wang, K.; He, T.; Wu, Y.; Wang, X. Mesoporous ZrO_2 Nanoframes for Biomass Upgrading. *ACS Appl. Mater. Interfaces* **2017**, *9*, 26897–26906. doi:10.1021/acsami.7b07567.
86. Xu, G.R.; Bai, J.; Jiang, J.X.; Lee, J.M.; Chen, Y. Polyethyleneimine functionalized platinum superstructures: Enhancing hydrogen evolution performance by morphological and interfacial control. *Chem. Sci.* **2017**, *8*, 8411–8418. doi:10.1039/C7SC04109H.
87. Xu, G.R.; Bai, J.; Yao, L.; Xue, Q.; Jiang, J.X.; Zeng, J.H.; Chen, Y.; Lee, J.M. Polyallylamine-Functionalized Platinum Tripods: Enhancement of Hydrogen Evolution Reaction by Proton Carriers. *ACS Catal.* **2017**, *7*, 452–458. doi:10.1021/acscatal.6b03049.
88. Xu, G.R.; Wang, B.; Zhu, J.Y.; Liu, F.Y.; Chen, Y.; Zeng, J.H.; Jiang, J.X.; Liu, Z.H.; Tang, Y.W.; Lee, J.M. Morphological and Interfacial Control of Platinum Nanostructures for Electrocatalytic Oxygen Reduction. *ACS Catal.* **2016**, *6*, 5260–5267. doi:10.1021/acscatal.6b01440.
89. Fang, Y.; Cao, D.; Shi, Y.; Guo, S.; Wang, Q.; Zhang, G.; Cui, P.; Cheng, S. Highly Porous Pt2Ir Alloy Nanocrystals as a Superior Catalyst with High-Efficiency C–C Bond Cleavage for Ethanol Electrooxidation. *J. Phys. Chem. Lett.* **2021**, *12*, 6773–6780.
90. Sadek, M.; Abd El-Lateef, H.M.; Mohran, H.S.; Elrouby, M. A promising star-like PtNi and coral reefs-like PtCo nano-structured materials for direct methanol fuel cell application. *Electrochim. Acta* **2021**, *399*, 139370.
91. Zhao, Y.; Wu, F.; Wei, J.; Sun, H.; Yuan, Y.; Bao, H.; Li, F.; Zhang, Z.; Han, S.; Niu, W. Designer Gold-Framed Palladium Nanocubes for Plasmon-Enhanced Electrocatalytic Oxidation of Ethanol. *Chem.—Eur. J.* **2022**. https://doi.org/10.1002/chem.202200494.
92. Hyun-Jung, C.; Kang, J.Y.; Jeon, I.Y.; Eo, S.M.; Tan, L.S.; Baek, J.B. Immobilization of platinum nanoparticles on 3,4-diaminobenzoyl-functionalized multi-walled carbon nanotube and its electrocatalytic activity. *J. Nanoparticle Res.* **2012**, *14*, 704. doi:10.1007/s11051-011-0704-5.
93. Loza, K.; Heggen, M.; Epple, M. Synthesis, Structure, Properties, and Applications of Bimetallic Nanoparticles of Noble Metals. *Adv. Funct. Mater.* **2020**, *30*, 1909260. doi:10.1002/adfm.201909260.
94. Pandey, P.C.; Mitra, M.D.; Shukla, S.; Narayan, R.J. Organotrialkoxysilane-Functionalized Noble Metal Monometallic, Bimetallic, and Trimetallic Nanoparticle Mediated Non-Enzymatic Sensing of Glucose by Resonance Rayleigh Scattering. *Biosensors* **2021**, *11*, 122. doi:10.3390/bios11040122.
95. Ali, S.; Sharma, A.S.; Ahmad, W.; Zareef, M.; Hassan, M.M.; Viswadevarayalu, A.; Jiao, T.; Li, H.; Chen, Q. Noble Metals Based Bimetallic and Trimetallic Nanoparticles: Controlled Synthesis, Antimicrobial and Anticancer Applications. *Crit. Rev. Anal. Chem.* **2021**, *51*, 454–481. doi:10.1080/10408347.2020.1743964.
96. Li, C.; Wang, H.; Li, Y.; Yu, H.; Yin, S.; Xue, H.; Li, X.; Xu, Y.; Wang, L. Tri-metallic PtPdAu mesoporous nanoelectrocatalysts. *Nanotechnology* **2018**, *29*, 255404. doi:10.1088/1361-6528/aabb47.
97. Rodrigues, T.S.; da Silva, A.G.M.; Camargo, P.H.C. Nanocatalysis by noble metal nanoparticles: Controlled synthesis for the optimization and understanding of activities. *J. Mater. Chem. A* **2019**, *7*, 5857–5874. doi:10.1039/C9TA00074G.
98. González, A.L.; Reyes-Esqueda, J.A.; Noguez, C. Optical Properties of Elongated Noble Metal Nanoparticles. *J. Phys. Chem. C* **2008**, *112*, 7356–7362. doi:10.1021/jp800432q.
99. Lee, J.H.; Choi, S.U.; Jang, S.P.; Lee, S.Y. Production of aqueous spherical gold nanoparticles using conventional ultrasonic bath. *Nanoscale Res. Lett.* **2012**, *7*, 420.
100. Murphy, C.J.; Sau, T.K.; Gole, A.M.; Orendorff, C.J.; Gao, J.; Gou, L.; Hunyadi, S.E.; Li, T. Anisotropic metal nanoparticles: Synthesis, assembly, and optical applications. *J. Phys. Chem. B* **2005**, *109*, 13857–13870.
101. Millstone, J.E.; Hurst, S.J.; Métraux, G.S.; Cutler, J.I.; Mirkin, C.A. Colloidal Gold and Silver Triangular Nanoprisms. *Small* **2009**, *5*, 646–664. doi:10.1002/smll.200801480.

102. Mulder, D.W.; Phiri, M.M.; Jordaan, A.; Vorster, B.C. Modified HEPES one-pot synthetic strategy for gold nanostars. *R. Soc. Open Sci.* **2019**, *6*, 190160. doi:10.1098/rsos.190160.
103. Wang, Y.; Zheng, Y.; Huang, C.Z.; Xia, Y. Synthesis of Ag Nanocubes 18–32 nm in Edge Length: The Effects of Polyol on Reduction Kinetics, Size Control, and Reproducibility. *J. Am. Chem. Soc.* **2013**, *135*, 1941–1951. doi:10.1021/ja311503q.
104. Jiu, J.; Murai, K.; Kim, D.; Kim, K.; Suganuma, K. Preparation of Ag nanorods with high yield by polyol process. *Mater. Chem. Phys.* **2009**, *114*, 333–338. doi:10.1016/j.matchemphys.2008.09.028.
105. Garcia-Leis, A.; Garcia-Ramos, J.V.; Sanchez-Cortes, S. Silver Nanostars with High SERS Performance. *J. Phys. Chem. C* **2013**, *117*, 7791–7795. doi:10.1021/jp401737y.
106. Zaheer, Z.; Rafiuddin. Multi-branched flower-like silver nanoparticles: Preparation and characterization. *Colloids Surf. Physicochem. Eng. Asp.* **2011**, *384*, 427–431. doi:10.1016/j.colsurfa.2011.04.030.
107. Bastús, N.G.; Merkoçi, F.; Piella, J.; Puntes, V. Synthesis of Highly Monodisperse Citrate-Stabilized Silver Nanoparticles of up to 200 nm: Kinetic Control and Catalytic Properties. *Chem. Mater.* **2014**, *26*, 2836–2846.
108. Nagao, H.; Ichiji, M.; Hirasawa, I. Synthesis of Platinum Nanoparticles by Reductive Crystallization Using Polyethyleneimine. *Chem. Eng. Technol.* **2017**, *40*, 1242–1246.
109. Herricks, T.; Chen, J.; Xia, Y. Polyol Synthesis of Platinum Nanoparticles: Control of Morphology with Sodium Nitrate. *Nano Letters* **2004**, *4*, 2367–2371.
110. Walbrück, K.; Kuellmer, F.; Witzleben, S.; Guenther, K. Synthesis and Characterization of PVP-Stabilized Palladium Nanoparticles by XRD, SAXS, SP-ICP-MS, and SEM. *J. Nanomater.* **2019**, *2019*, 4758108.
111. Iben Ayad, A.; Belda Marín, C.; Colaco, E.; Lefevre, C.; Méthivier, C.; Ould Driss, A.; Landoulsi, J.; Guénin, E. "Water soluble" palladium nanoparticle engineering for C–C coupling, reduction and cyclization catalysis. *Green Chem.* **2019**, *21*, 6646–6657. doi:10.1039/C9GC02546D.
112. Wang, Y.; Du, M.; Xu, J.; Yang, P.; Du, Y. Size-Controlled Synthesis of Palladium Nanoparticles. *J. Dispers. Sci. Technol.* **2008**, *29*, 891–894. doi:10.1080/01932690701783499.
113. Alsalahi, W.; Tylus, W.; Trzeciak, A.M. Green synthesis of rhodium nanoparticles, catalytically active in benzene hydrogenation and 1-hexene hydroformylation. *ChemCatChem* **2018**, *10*, 2051–2058.
114. Fernández, G.; Pleixats, R. Rhodium Nanoparticles Stabilized by PEG-Tagged Imidazolium Salts as Recyclable Catalysts for the Hydrosilylation of Internal Alkynes and the Reduction of Nitroarenes. *Catalysts* **2020**, *10*, 1195.
115. Biacchi, A.J.; Schaak, R.E. Ligand-Induced Fate of Embryonic Species in the Shape-Controlled Synthesis of Rhodium Nanoparticles. *ACS Nano* **2015**, *9*, 1707–1720. doi:10.1021/nn506517e.
116. Yu, M.; Diao, X.; Huang, T.; Liu, H.; Li, J. Shape-controlled Synthesis of Ruthenium Nanoparticles. *Funct. Mater. Lett.* **2011**, *4*, 337–340.
117. Yan, X.; Liu, H.; Liew, K.Y. Size control of polymer-stabilized ruthenium nanoparticles by polyol reduction. *J. Mater. Chem.* **2001**, *11*, 3387–3391.
118. Kusada, K.; Kobayashi, H.; Yamamoto, T.; Matsumura, S.; Sumi, N.; Sato, K.; Nagaoka, K.; Kubota, Y.; Kitagawa, H. Discovery of Face-Centered-Cubic Ruthenium Nanoparticles: Facile Size-Controlled Synthesis Using the Chemical Reduction Method. *J. Am. Chem. Soc.* **2013**, *135*, 5493–5496. doi:10.1021/ja311261s.
119. Cui, M.; Zhao, Y.; Wang, C.; Song, Q. Synthesis of 2.5 nm colloidal iridium nanoparticles with strong surface enhanced Raman scattering activity. *Microchim. Acta* **2016**, *183*, 2047–2053.
120. Bonet, F.; Delmas, V.; Grugeon, S.; Herrera Urbina, R.; Silvert, P.Y.; Tekaia-Elhsissen, K. Synthesis of monodisperse Au, Pt, Pd, Ru and Ir nanoparticles in ethylene glycol. *Nanostructured Mater.* **1999**, *11*, 1277–1284. doi:10.1016/S0965-9773(99)00419-5.
121. Chakrapani, K.; Sampath, S. Interconnected, ultrafine osmium nanoclusters: Preparation and surface enhanced Raman scattering activity. *Chem. Commun.* **2013**, *49*, 6173–6175. doi:10.1039/C3CC41940A.
122. Wakisaka, T.; Kusada, K.; Yamamoto, T.; Toriyama, T.; Matsumura, S.; Ibrahima, G.; Seo, O.; Kim, J.; Hiroi, S.; Sakata, O.; et al. Discovery of face-centred cubic Os nanoparticles. *Chem. Commun.* **2020**, *56*, 372–374. doi:10.1039/C9CC09192K.
123. Huang, X.; Qi, X.; Huang, Y.; Li, S.; Xue, C.; Gan, C.L.; Boey, F.; Zhang, H. Photochemically Controlled Synthesis of Anisotropic Au Nanostructures: Platelet-like Au Nanorods and Six-Star Au Nanoparticles. *ACS Nano* **2010**, *4*, 6196–6202. doi:10.1021/nn101803m.
124. Guo, S.; Wang, E. Noble metal nanomaterials: Controllable synthesis and application in fuel cells and analytical sensors. *Nano Today* **2011**, *6*, 240–264. doi:10.1016/j.nantod.2011.04.007.
125. Xing, L.; Xiahou, Y.; Zhang, P.; Du, W.; Xia, H. Size control synthesis of monodisperse, quasi-spherical silver nanoparticles to realize surface-enhanced Raman scattering uniformity and reproducibility. *ACS Appl. Mater. Interfaces* **2019**, *11*, 17637–17646.
126. Sarfo, D.K.; Izake, E.L.; O'Mullane, A.P.; Ayoko, G.A. Fabrication of nanostructured SERS substrates on conductive solid platforms for environmental application. *Crit. Rev. Environ. Sci. Technol.* **2019**, *49*, 1294–1329.
127. Gong, L.; Wang, Y.; Liu, J. Bioapplications of renal-clearable luminescent metal nanoparticles. *Biomater. Sci.* **2017**, *5*, 1393–1406.
128. Elahi, N.; Kamali, M.; Baghersad, M.H. Recent biomedical applications of gold nanoparticles: A review. *Talanta* **2018**, *184*, 537–556.
129. Kowalczyk, P.; Szymczak, M.; Maciejewska, M.; Laskowski, Ł.; Laskowska, M.; Ostaszewski, R.; Skiba, G.; Franiak-Pietryga, I. All that glitters is not silver—A new look at microbiological and medical applications of silver nanoparticles. *Int. J. Mol. Sci.* **2021**, *22*, 854.
130. Prasher, P.; Singh, M.; Mudila, H. Silver nanoparticles as antimicrobial therapeutics: Current perspectives and future challenges. *3 Biotech* **2018**, *8*, 1–23.

131. Bai, Q.; Li, D.; He, L.; Xiao, H.; Sui, N.; Liu, M. Solvent-free selective hydrogenation of o-chloronitrobenzene to o-chloroaniline over alumina supported Pt nanoparticles. *Prog. Nat. Sci. Mater. Int.* **2015**, *25*, 179–184.
132. Lin, L.; Zhou, W.; Gao, R.; Yao, S.; Zhang, X.; Xu, W.; Zheng, S.; Jiang, Z.; Yu, Q.; Li, Y.W.; et al. Low-temperature hydrogen production from water and methanol using Pt/α-MoC catalysts. *Nature* **2017**, *544*, 80–83.
133. Li, N.; Tang, S.; Meng, X. Preparation of Pt–GO composites with high-number-density Pt nanoparticles dispersed uniformly on GO nanosheets. *Prog. Nat. Sci. Mater. Int.* **2016**, *26*, 139–144.
134. Rong, H.; Zhang, S.; Muhammad, S.; Zhang, J. Noble metal-based nanocomposites for fuel cells. *Novel Nanomaterials*; IntechOpen: London, UK, 2018; pp. 291–310.
135. Chaturvedi, S.; Dave, P.N. A review on the use of nanometals as catalysts for the thermal decomposition of ammonium perchlorate. *J. Saudi Chem. Soc.* **2013**, *17*, 135–149.
136. Zhao, P.; Feng, X.; Huang, D.; Yang, G.; Astruc, D. Basic concepts and recent advances in nitrophenol reduction by gold-and other transition metal nanoparticles. *Coord. Chem. Rev.* **2015**, *287*, 114–136.
137. Cuenya, B.R.; Behafarid, F. Nanocatalysis: Size-and shape-dependent chemisorption and catalytic reactivity. *Surf. Sci. Rep.* **2015**, *70*, 135–187.
138. Bond, G.C. Supported metal catalysts: Some unsolved problems. *Chem. Soc. Rev.* **1991**, *20*, 441–475. doi:10.1039/CS9912000441.
139. Geonmonond, R.; Marques da Silva, A.; Camargo, P. Controlled synthesis of noble metal nanomaterials: Motivation, principles, and opportunities in nanocatalysis. *Anais Academia Brasileira Ciências* **2018**, *90*, 719–744. doi:10.1590/0001-3765201820170561.
140. Pradeep, T.; Anshup. Noble metal nanoparticles for water purification: A critical review. *Thin Solid Films* **2009**, *517*, 6441–6478. doi:10.1016/j.tsf.2009.03.195.
141. Lee, S.; Fan, C.; Wu, T.; Anderson, S.L. CO Oxidation on Aun/TiO_2 Catalysts Produced by Size-Selected Cluster Deposition. *J. Am. Chem. Soc.* **2004**, *126*, 5682–5683. doi:10.1021/ja049436v.
142. Yu, K.; Yeung, C.; Tsang, S. Carbon Dioxide Fixation into Chemicals (Methyl Formate) at High Yields by Surface Coupling over a Pd/Cu/ZnO Nanocatalyst. *J. Am. Chem. Soc.* **2007**, *129*, 6360–1. doi:10.1021/ja0706302.
143. Li, B.; Lu, G.; Zhou, X.; Cao, X.; Boey, F.; Zhang, H. Controlled Assembly of Gold Nanoparticles and Graphene Oxide Sheets on Dip Pen Nanolithography-Generated Templates. *Langmuir* **2009**, *25*, 10455–10458. doi:10.1021/la902601v.
144. Li, L.; Xing, Y. Pt-Ru Nanoparticles Supported on Carbon Nanotubes as Methanol Fuel Cell Catalysts. *J. Phys. Chem. C* **2007**, *111*, 2803–2808. doi:10.1021/jp0655470.
145. Zhou, W.; Du, G.; Hu, P.; Yin, Y.; Li, J.; Yu, J.; Wang, G.; Wang, J.; Liu, H.; Wang, J.; et al. Nanopaper based on Ag/TiO2 nanobelts heterostructure for continuous-flow photocatalytic treatment of liquid and gas phase pollutants. *J. Hazard. Mater.* **2011**, *197*, 19–25. doi:10.1016/j.jhazmat.2011.09.051.
146. Ishida, H.; Campbell, S.; Blackwell, J. General Approach to Nanocomposite Preparation. *Chem. Mater.* **2000**, *12*, 1260–1267. doi:10.1021/cm990479y.
147. Rahmati, S.; Doherty, W.; Amani Babadi, A.; Akmal Che Mansor, M.S.; Julkapli, N.M.; Hessel, V.; Ostrikov, K.K. Gold–Carbon Nanocomposites for Environmental Contaminant Sensing. *Micromachines* **2021**, *12*, 719. doi:10.3390/mi12060719.
148. Rice, P.; Hu, P. Understanding supported noble metal catalysts using first-principles calculations. *J. Chem. Phys.* **2019**, *151*, 180902. doi:10.1063/1.5126090.
149. Subramanian, V.; Wolf, E.E.; Kamat, P.V. Catalysis with TiO_2/Gold Nanocomposites. Effect of Metal Particle Size on the Fermi Level Equilibration. *J. Am. Chem. Soc.* **2004**, *126*, 4943–4950. doi:10.1021/ja0315199.
150. Richter, F.; Meng, Y.; Klasen, T.; Sahraoui, L.; Schüth, F. Structural mimicking of inorganic catalyst supports with polydivinylbenzene to improve performance in the selective aerobic oxidation of ethanol and glycerol in water. *J. Catal.* **2013**, *308*, 341–351. doi:10.1016/j.jcat.2013.08.014.
151. Martinuzzi, S.; Cozzula, D.; Centomo, P.; Zecca, M.; Müller, T.E. The distinct role of the flexible polymer matrix in catalytic conversions over immobilised nanoparticles. *RSC Adv.* **2015**, *5*, 56181–56188. doi:10.1039/C5RA05061H.
152. Koga, H.; Tokunaga, E.; Hidaka, M.; Umemura, Y.; Saito, T.; Isogai, A.; Kitaoka, T. Topochemical synthesis and catalysis of metal nanoparticles exposed on crystalline cellulose nanofibers. *Chem. Commun.* **2010**, *46*, 8567–8569. doi:10.1039/C0CC02754E.
153. Turner, M.; Golovko, V.; Vaughan, O.; Abdulkin, P.; Berenguer-Murcia, A.; Tikhov, M.; Johnson, B.; Lambert, R. Selective oxidation with dioxygen by gold nanoparticle catalysts derived from 55-atom clusters. *Nature* **2008**, *454*, 981–983. doi:10.1038/nature07194.
154. Yamada, Y.; Tsung, C.K.; Huang, W.; Huo, Z.; Habas, S.; Soejima, T.; Aliaga, C.; Somorjai, G.; Yang, P. Nanocrystal bilayer for tandem catalysis. *Nat. Chem.* **2011**, *3*, 372–376. doi:10.1038/nchem.1018.
155. An, K.; Alayoglu, S.; Musselwhite, N.; Na, K.; Somorjai, G.A. Designed Catalysts from Pt Nanoparticles Supported on Macroporous Oxides for Selective Isomerization of n-Hexane. *J. Am. Chem. Soc.* **2014**, *136*, 6830–6833. doi:10.1021/ja5018656.
156. Kuo, C.H.; Tang, Y.; Chou, L.Y.; Sneed, B.T.; Brodsky, C.N.; Zhao, Z.; Tsung, C.K. Yolk–Shell Nanocrystal@ZIF-8 Nanostructures for Gas-Phase Heterogeneous Catalysis with Selectivity Control. *J. Am. Chem. Soc.* **2012**, *134*, 14345–14348. doi:10.1021/ja306869j.
157. Joo, S.H.; Park, J.; Tsung, C.K.; Yamada, Y.; Yang, P.; Somorjai, G. Thermally Stable Pt/Mesoporous Silica Core-shell Nanocatalysts for High-Temperature Reactions. *Nat. Mater.* **2008**, *8*, 126–31. doi:10.1038/nmat2329.
158. Wang, S.; Wang, J.; Zhao, Q.; Li, D.; Wang, J.Q.; Cho, M.; Cho, H.; Terasaki, O.; Chen, S.; Wan, Y. Highly Active Heterogeneous 3 nm Gold Nanoparticles on Mesoporous Carbon as Catalysts for Low-Temperature Selective Oxidation and Reduction in Water. *ACS Catal.* **2015**, *5*, 797–802. doi:10.1021/cs501896c.

159. Lam, E.; Luong, J.H. Carbon Materials as Catalyst Supports and Catalysts in the Transformation of Biomass to Fuels and Chemicals. *ACS Catal.* **2014**, *4*, 3393–3410. doi:10.1021/cs5008393.
160. Zhou, R.; Qiao, S. Silver/Nitrogen-Doped Graphene Interaction and Its Effect on Electrocatalytic Oxygen Reduction. *Chem. Mater.* **2014**, *26*, 5868–5873. doi:10.1021/cm502260m.
161. Zheng, Y.; Luo, R.; Xu, Y.; Zhang, L.; Liu, P.; Chen, Q. Adsorbate-Mediated Deposition of Noble-Metal Nanoparticles on Carbon Substrates for Electrocatalysis. *ACS Appl. Energy Mater.* **2020**, *3*, 6460–6465. doi:10.1021/acsaem.0c00706.
162. Frackowiak, E.; Beguin, F. Carbon materials for the electrochemical storage of energy in capacitors. *Carbon* **2001**, *39*, 937–950.
163. Yang, T.; Ling, H.; Lamonier, J.F.; Jaroniec, M.; Huang, J.; Monteiro, M.J.; Liu, J. A synthetic strategy for carbon nanospheres impregnated with highly monodispersed metal nanoparticles. *NPG Asia Mater.* **2016**, *8*, e240–e240.
164. Dai, L.; Chang, D.W.; Baek, J.B.; Lu, W. Carbon nanomaterials: Carbon nanomaterials for advanced energy conversion and storage (small 8/2012). *Small* **2012**, *8*, 1122–1122.
165. Noor, T.; Yaqoob, L.; Iqbal, N. Recent Advances in Electrocatalysis of Oxygen Evolution Reaction using Noble-Metal, Transition-Metal, and Carbon-Based Materials. *ChemElectroChem* **2021**, *8*, 447–483.
166. Dai, L.; Xue, Y.; Qu, L.; Choi, H.J.; Baek, J.B. Metal-free catalysts for oxygen reduction reaction. *Chem. Rev.* **2015**, *115*, 4823–4892.
167. Liu, H.; Song, C.; Zhang, L.; Zhang, J.; Wang, H.; Wilkinson, D.P. A review of anode catalysis in the direct methanol fuel cell. *J. Power Sources* **2006**, *155*, 95–110.
168. Uchida, M.; Aoyama, Y.; Tanabe, M.; Yanagihara, N.; Eda, N.; Ohta, A. Influences of both carbon supports and heat-treatment of supported catalyst on electrochemical oxidation of methanol. *J. Electrochem. Soc.* **1995**, *142*, 2572.
169. Liu, Y.; Ji, C.; Gu, W.; Jorne, J.; Gasteiger, H.A. Effects of catalyst carbon support on proton conduction and cathode performance in PEM fuel cells. *J. Electrochem. Soc.* **2011**, *158*, B614.
170. Qu, W.L.; Wang, Z.B.; Jiang, Z.Z.; Gu, D.M.; Yin, G.P. Investigation on performance of Pd/Al_2O_3-C catalyst synthesized by microwave assisted polyol process for electrooxidation of formic acid. *Rsc Adv.* **2012**, *2*, 344–350.
171. Moore, A.D.; Holmes, S.M.; Roberts, E.P. Evaluation of porous carbon substrates as catalyst supports for the cathode of direct methanol fuel cells. *RSC Adv.* **2012**, *2*, 1669–1674.
172. Vogel, W. Size contraction in Pt/C and PtRu/C commercial E-TEK electrocatalysts: An in situ X-ray diffraction study. *J. Phys. Chem. C* **2008**, *112*, 13475–13482.
173. Chen, T.W.; Kalimuthu, P.; Veerakumar, P.; Lin, K.C.; Chen, S.M.; Ramachandran, R.; Mariyappan, V.; Chitra, S. Recent Developments in Carbon-Based Nanocomposites for Fuel Cell Applications: A Review. *Molecules* **2022**, *27*, 761.
174. Li, J.; Stephanopoulos, M.F.; Xia, Y. Introduction: Heterogeneous single-atom catalysis. *Chem. Rev.* **2020**, *120*, 11699–11702.
175. Wang, A.; Li, J.; Zhang, T. Heterogeneous single-atom catalysis. *Nat. Rev. Chem.* **2018**, *2*, 65–81.
176. Wu, B.; Kuang, Y.; Zhang, X.; Chen, J. Noble metal nanoparticles/carbon nanotubes nanohybrids: Synthesis and applications. *Nano Today* **2011**, *6*, 75–90.
177. Khalil, I.; Julkapli, N.M.; Yehye, W.A.; Basirun, W.J.; Bhargava, S.K. Graphene–gold nanoparticles hybrid—synthesis, functionalization, and application in a electrochemical and surface-enhanced raman scattering biosensor. *Materials* **2016**, *9*, 406.
178. Chung, S.; Ham, K.; Kang, S.; Ju, H.; Lee, J. Enhanced corrosion tolerance and highly durable ORR activity by low Pt electrocatalyst on unique pore structured CNF in PEM fuel cell. *Electrochim. Acta* **2020**, *348*, 136346. doi:10.1016/j.electacta.2020.136346.
179. Jeon, Y.; Ji, Y.; Cho, Y.I.; Lee, C.; Park, D.H.; Shul, Y.G. Oxide–Carbon Nanofibrous Composite Support for a Highly Active and Stable Polymer Electrolyte Membrane Fuel-Cell Catalyst. *ACS Nano* **2018**, *12*, 6819–6829. doi:10.1021/acsnano.8b02040.
180. Ott, S.; Orfanidi, A.; Schmies, H.; Anke, B.; Nong, H.N.; Hübner, J.; Gernert, U.; Gliech, M.; Lerch, M.; Strasser, P. Ionomer distribution control in porous carbon-supported catalyst layers for high-power and low Pt-loaded proton exchange membrane fuel cells. *Nat. Mater.* **2020**, *19*, 77–85.
181. Mardle, P.; Ji, X.; Wu, J.; Guan, S.; Dong, H.; Du, S. Thin film electrodes from Pt nanorods supported on aligned N-CNTs for proton exchange membrane fuel cells. *Appl. Catal. B Environ.* **2020**, *260*, 118031.
182. Orfanidi, A.; Madkikar, P.; El-Sayed, H.A.; Harzer, G.S.; Kratky, T.; Gasteiger, H.A. The Key to High Performance Low Pt Loaded Electrodes. *J. Electrochem. Soc.* **2017**, *164*, F418–F426. doi:10.1149/2.1621704jes.
183. Du, S.; Lu, Y.; Steinberger-Wilckens, R. PtPd nanowire arrays supported on reduced graphene oxide as advanced electrocatalysts for methanol oxidation. *Carbon* **2014**, *79*, 346–353. doi:10.1016/j.carbon.2014.07.076.
184. Zhang, X.; Yang, P.; Jiang, S.P. Pd nanoparticles assembled on Ni- and N-doped carbon nanotubes towards superior electrochemical activity. *Int. J. Hydrogen Energy* **2021**, *46*, 2065–2074. doi:10.1016/j.ijhydene.2020.10.096.
185. Tetrahydrofuran-functionalized multi-walled carbon nanotubes as effective support for Pt and PtSn electrocatalysts of fuel cells. *Electrochim. Acta* **2010**, *55*, 2964–2971. doi:10.1016/j.electacta.2010.01.031.
186. Alegre, C.; Gálvez, M.E.; Baquedano, E.; Moliner, R.; Pastor, E.; Lázaro, M.J. Oxygen-Functionalized Highly Mesoporous Carbon Xerogel Based Catalysts for Direct Methanol Fuel Cell Anodes. *J. Phys. Chem. C* **2013**, *117*, 13045–13058. doi:10.1021/jp400824n.
187. La-Torre-Riveros, L.; Guzman-Blas, R.; Méndez-Torres, A.E.; Prelas, M.; Tryk, D.A.; Cabrera, C.R. Diamond Nanoparticles as a Support for Pt and PtRu Catalysts for Direct Methanol Fuel Cells. *ACS Appl. Mater. Interfaces* **2012**, *4*, 1134–1147. doi:10.1021/am2018628.
188. Beltrán-Gastélum, M.; Salazar-Gastélum, M.; Flores-Hernández, J.; Botte, G.; Pérez-Sicairos, S.; Romero-Castañon, T.; Reynoso-Soto, E.; Félix-Navarro, R. Pt-Au nanoparticles on graphene for oxygen reduction reaction: Stability and performance on proton exchange membrane fuel cell. *Energy* **2019**, *181*, 1225–1234. doi:10.1016/j.energy.2019.06.033.

189. Şanlı, L.I.; Yarar, B.; Bayram, V.; Gürsel, S.A. Electrosprayed catalyst layers based on graphene–carbon black hybrids for the next-generation fuel cell electrodes. *J. Mater. Sci.* **2017**, *52*, 2091–2102. doi:10.1007/s10853-016-0497-0.
190. Zhou, Y.; Hu, X.; Guo, S.; Yu, C.; Zhong, S.; Liu, X. Multi-functional graphene/carbon nanotube aerogels for its applications in supercapacitor and direct methanol fuel cell. *Electrochim. Acta* **2018**, *264*, 12–19. doi:10.1016/j.electacta.2018.01.009.
191. Chen, D.J.; Zhang, Q.; Feng, J.X.; Ju, K.J.; Wang, A.J.; Wei, J.; Feng, J.J. One-pot wet-chemical co-reduction synthesis of bimetallic gold–platinum nanochains supported on reduced graphene oxide with enhanced electrocatalytic activity. *J. Power Sources* **2015**, *287*, 363–369. doi:10.1016/j.jpowsour.2015.04.080.
192. Pan, D.; Li, X.; Zhang, A. Platinum assisted by carbon quantum dots for methanol electro-oxidation. *Appl. Surf. Sci.* **2018**, *427*, 715–723. doi:10.1016/j.apsusc.2017.09.060.
193. Deming, C.P.; Mercado, R.; Lu, J.E.; Gadiraju, V.; Khan, M.; Chen, S. Oxygen Electroreduction Catalyzed by Palladium Nanoparticles Supported on Nitrogen-Doped Graphene Quantum Dots: Impacts of Nitrogen Dopants. *ACS Sustain. Chem. Eng.* **2016**, *4*, 6580–6589. doi:10.1021/acssuschemeng.6b01476.
194. Zhang, M.; Li, H.; Chen, J.; Yi, L.; Shao, P.; Xu, C.Y.; Wen, Z. Nitrogen-doped graphite encapsulating RuCo nanoparticles toward high-activity catalysis of water oxidation and reduction. *Chem. Eng. J.* **2021**, *422*, 130077. doi:10.1016/j.cej.2021.130077.
195. Mondal, S.K. Synthesis of Mesoporous Fullerene and its Platinum Composite: A Catalyst for PEMFc. *J. Electrochem. Soc.* **2012**, *159*, K156–K160. doi:10.1149/2.003206jes.
196. McPherson, I.J.; Ash, P.A.; Jones, L.; Varambhia, A.; Jacobs, R.M.J.; Vincent, K.A. Electrochemical CO Oxidation at Platinum on Carbon Studied through Analysis of Anomalous in Situ IR Spectra. *J. Phys. Chem. C* **2017**, *121*, 17176–17187. doi:10.1021/acs.jpcc.7b02166.
197. Zhang, X.; Zhang, J.W.; Xiang, P.H.; Qiao, J. Fabrication of graphene-fullerene hybrid by self-assembly and its application as support material for methanol electrocatalytic oxidation reaction. *Appl. Surf. Sci.* **2018**, *440*, 477–483. doi:10.1016/j.apsusc.2018.01.150.
198. Gu, K.; Kim, E.; Sharma, S.; Sharma, P.; Bliznakov, S.; Hsiao, B.; Rafailovich, M. Mesoporous carbon aerogel with tunable porosity as the catalyst support for enhanced proton-exchange membrane fuel cell performance. *Mater. Today Energy* **2021**, *19*, 100560.
199. Kin, Y.; Saito, K.; Oda, H.; Ando, T.; Nakagawa, K. Development of Direct Methanol Fuel Cell Catalyst Using Marimo Nano Carbon. *Catal. Lett.* **2019**, *149*, 1–6. doi:10.1007/s10562-018-2588-9.
200. Bak, J.; Kim, H.; Lee, S.; Kim, M.; Kim, E.J.; Roh, J.; Shin, J.; Choi, C.H.; Cho, E. Boosting the Role of Ir in Mitigating Corrosion of Carbon Support by Alloying with Pt. *ACS Catal.* **2020**, *10*, 12300–12309. doi:10.1021/acscatal.0c02845.
201. Luo, F.; Hu, H.; Zhao, X.; Yang, Z.; Zhang, Q.; Xu, J.; Kaneko, T.; Yoshida, Y.; Zhu, C.; Cai, W. Robust and Stable Acidic Overall Water Splitting on Ir Single Atoms. *Nano Lett.* **2020**, *20*, 2120–2128. doi:10.1021/acs.nanolett.0c00127.
202. Choudhary, A.K.; Pramanik, H. Addition of rhenium (Re) to Pt-Ru/f-MWCNT anode electrocatalysts for enhancement of ethanol electrooxidation in half cell and single direct ethanol fuel cell. *Int. J. Hydrogen Energy* **2020**, *45*, 13300–13321. doi:10.1016/j.ijhydene.2020.03.044.
203. Tsai, M.C.; Yeh, T.K.; Tsai, C.H. Electrodeposition of platinum-ruthenium nanoparticles on carbon nanotubes directly grown on carbon cloths for methanol oxidation. *Mater. Chem. Phys.* **2008**, *109*, 422–428. doi:10.1016/j.matchemphys.2007.12.010.
204. Zhou, Y.G.; Chen, J.J.; Wang, F.b.; Sheng, Z.H.; Xia, X.H. A facile approach to the synthesis of highly electroactive Pt nanoparticles on graphene as an anode catalyst for direct methanol fuel cells. *Chem. Commun.* **2010**, *46*, 5951–5953.
205. Yao, Z.; Zhu, M.; Jiang, F.; Du, Y.; Wang, C.; Yang, P. Highly efficient electrocatalytic performance based on Pt nanoflowers modified reduced graphene oxide/carbon cloth electrode. *J. Mater. Chem.* **2012**, *22*, 13707–13713. doi:10.1039/C2JM31683H.
206. Ahn, S.H.; Choi, I.; Kwon, O.J.; Kim, J. One-step co-electrodeposition of Pt-Ru electrocatalysts on carbon paper for direct methanol fuel. *Chem. Eng. J.* **2012**, *s 181–182*, 276–280. doi:10.1016/j.cej.2011.11.079.
207. Gao, L.; Ding, L.; Fan, L. Pt nanoflower/graphene-layered composites by ZnO nanoparticle expansion of graphite and their enhanced electrocatalytic activity for methanol oxidation. *Electrochim. Acta* **2013**, *106*, 159–164. doi:10.1016/j.electacta.2013.05.065.
208. Gao, F.; Yang, N.; Smirnov, W.; Obloh, H.; Nebel, C. Size-controllable and homogeneous platinum nanoparticles on diamond using wet chemically assisted electrodeposition. *Electrochim. Acta* **2013**, *90*, 445–451. doi:10.1016/j.electacta.2012.12.050.
209. Mavrokefalos, C.; Hasan, M.; Rohan, J.; Foord, J. Enhanced Mass Activity and Stability of Bimetallic Pd-Ni Nanoparticles on Boron-Doped Diamond for Direct Ethanol Fuel Cell Applications. *ChemElectroChem* **2017**, *5*, 455–463. doi:10.1002/celc.201701105.
210. Dhanasekaran, P.; Lokesh, K.; Ojha, P.; Sahu, A.; Bhat, S.; Kalpana, D. Electrochemical deposition of three-dimensional platinum nanoflowers for high-performance polymer electrolyte fuel cells. *J. Colloid Interface Sci.* **2020**, *572*, 198–206. doi:10.1016/j.jcis.2020.03.078.
211. Goh, Y.A.; Chen, X.; Yasin, F.M.; Eggers, P.K.; Boulos, R.A.; Wang, X.; Chua, H.T.; Raston, C.L. Shear flow assisted decoration of carbon nano-onions with platinum nanoparticles. *Chem. Commun.* **2013**, *49*, 5171–5173. doi:10.1039/C3CC41647J.
212. Wang, Q.; Geng, B.; Tao, B. A facile room temperature chemical route to Pt nanocube/carbon nanotube heterostructures with enhanced electrocatalysis. *J. Power Sources* **2011**, *196*, 191–195. doi:10.1016/j.jpowsour.2010.06.035.
213. Chen, X.; Hou, Y.; Wang, H.; Cao, Y.; He, J. Facile Deposition of Pd Nanoparticles on Carbon Nanotube Microparticles and Their Catalytic Activity for Suzuki Coupling Reactions. *J. Phys. Chem. C* **2008**, *112*, 8172–8176. doi:10.1021/jp800610q.
214. Qu, L.; Dai, L. Substrate-Enhanced Electroless Deposition of Metal Nanoparticles on Carbon Nanotubes. *J. Am. Chem. Soc.* **2005**, *127*, 10806–10807. doi:10.1021/ja053479+.

215. Ming, M.; Zhang, Y.; He, C.; Zhao, L.; Niu, S.; Fan, G.; Hu, J.S. Room-Temperature Sustainable Synthesis of Selected Platinum Group Metal (PGM = Ir, Rh, and Ru) Nanocatalysts Well-Dispersed on Porous Carbon for Efficient Hydrogen Evolution and Oxidation. *Small* **2019**, *15*, 1903057. doi:10.1002/smll.201903057.
216. Bian, Y.; Wang, H.; Gao, Z.; Hu, J.; Liu, D.; Dai, L. A facile approach to high-performance trifunctional electrocatalysts by substrate-enhanced electroless deposition of Pt/NiO/Ni on carbon nanotubes. *Nanoscale* **2020**, *12*, 14615–14625. doi:10.1039/D0NR03378B.
217. Bahr, J.L.; Tour, J.M. Covalent chemistry of single-wall carbon nanotubes. *J. Mater. Chem.* **2002**, *12*, 1952–1958.
218. Jiang, L.; Gao, L. Modified carbon nanotubes: An effective way to selective attachment of gold nanoparticles. *Carbon* **2003**, *41*, 2923–2929.
219. Georgakilas, V.; Perman, J.A.; Tucek, J.; Zboril, R. Broad family of carbon nanoallotropes: Classification, chemistry, and applications of fullerenes, carbon dots, nanotubes, graphene, nanodiamonds, and combined superstructures. *Chem. Rev.* **2015**, *115*, 4744–4822.
220. Labulo, A.H.; Martincigh, B.S.; Omondi, B.; Nyamori, V.O. Advances in carbon nanotubes as efficacious supports for palladium-catalysed carbon–carbon cross-coupling reactions. *J. Mater. Sci.* **2017**, *52*, 9225–9248.
221. Zhang, R.Y.; Olin, H. Gold-carbon nanotube nanocomposites: Synthesis and applications. *Int. J. Biomed. Nanosci. Nanotechnol.* **2011**, *2*, 112–135.
222. Huang, H.; Wang, X. Recent progress on carbon-based support materials for electrocatalysts of direct methanol fuel cells. *J. Mater. Chem. A* **2014**, *2*, 6266–6291.
223. Li, H.; Chang, G.; Zhang, Y.; Tian, J.; Liu, S.; Luo, Y.; Asiri, A.M.; Al-Youbi, A.O.; Sun, X. Photocatalytic synthesis of highly dispersed Pd nanoparticles on reduced graphene oxide and their application in methanol electro-oxidation. *Catal. Sci. Technol.* **2012**, *2*, 1153–1156.
224. Fan, J.J.; Fan, Y.J.; Wang, R.X.; Xiang, S.; Tang, H.G.; Sun, S.G. A novel strategy for the synthesis of sulfur-doped carbon nanotubes as a highly efficient Pt catalyst support toward the methanol oxidation reaction. *J. Mater. Chem. A* **2017**, *5*, 19467–19475.
225. Lu, R.; Zang, J.; Wang, Y.; Zhao, Y. Microwave synthesis and properties of nanodiamond supported PtRu electrocatalyst for methanol oxidation. *Electrochim. Acta* **2012**, *60*, 329–333.
226. Hsieh, C.T.; Hung, W.M.; Chen, W.Y.; Lin, J.Y. Microwave-assisted polyol synthesis of Pt–Zn electrocatalysts on carbon nanotube electrodes for methanol oxidation. *Int. J. Hydrogen Energy* **2011**, *36*, 2765–2772.
227. Hsieh, C.T.; Wei, J.M.; Hsiao, H.T.; Chen, W.Y. Fabrication of flower-like platinum clusters onto graphene sheets by pulse electrochemical deposition. *Electrochim. Acta* **2012**, *64*, 177–182. doi:10.1016/j.electacta.2012.01.006.
228. He, Z.; Chen, J.; Liu, D.; Zhou, H.; Kuang, Y. Electrodeposition of Pt-Ru nanoparticles on carbon nanotubes and their electrocatalytic properties for methanol electrooxidation. *Diam. Relat. Mater.* **2004**, *13*, 1764–1770. doi:10.1016/j.diamond.2004.03.004.
229. Choi, H.C.; Shim, M.; Bangsaruntip, S.; Dai, H. Spontaneous Reduction of Metal Ions on the Sidewalls of Carbon Nanotubes. *J. Am. Chem. Soc.* **2002**, *124*, 9058–9059. doi:10.1021/ja026824t.
230. Shen, X.; Xia, X.; Du, Y.; Wang, C. Electroless deposition of Au nanoparticles on reduced graphene oxide/polyimide film for electrochemical detection of hydroquinone and catechol. *Front. Mater. Sci.* **2017**, *11*, 262–270.
231. Liu, X.W.; Mao, J.J.; Liu, P.D.; Wei, X.W. Fabrication of metal-graphene hybrid materials by electroless deposition. *Carbon* **2011**, *49*, 477–483. doi:10.1016/j.carbon.2010.09.044.
232. Qi, J.; Jiang, L.; Tang, Q.; Zhu, S.; Wang, S.; Yi, B.; Sun, G. Synthesis of graphitic mesoporous carbons with different surface areas and their use in direct methanol fuel cells. *Carbon* **2012**, *50*, 2824–2831.
233. Calvillo, L.; Celorrio, V.; Moliner, R.; Garcia, A.; Caméan, I.; Lazaro, M. Comparative study of Pt catalysts supported on different high conductive carbon materials for methanol and ethanol oxidation. *Electrochim. Acta* **2013**, *102*, 19–27.
234. Cao, J.; Chen, Z.; Xu, J.; Wang, W.; Chen, Z. Mesoporous carbon synthesized from dual colloidal silica/block copolymer template approach as the support of platinum nanoparticles for direct methanol fuel cells. *Electrochim. Acta* **2013**, *88*, 184–192.
235. Yarlagadda, V.; Carpenter, M.K.; Moylan, T.E.; Kukreja, R.S.; Koestner, R.; Gu, W.; Thompson, L.; Kongkanand, A. Boosting fuel cell performance with accessible carbon mesopores. *ACS Energy Lett.* **2018**, *3*, 618–621.
236. Maiyalagan, T.; Alaje, T.O.; Scott, K. Highly stable Pt–Ru nanoparticles supported on three-dimensional cubic ordered mesoporous carbon (Pt–Ru/CMK-8) as promising electrocatalysts for methanol oxidation. *J. Phys. Chem. C* **2012**, *116*, 2630–2638.
237. Su, F.; Poh, C.K.; Tian, Z.; Xu, G.; Koh, G.; Wang, Z.; Liu, Z.; Lin, J. Electrochemical behavior of Pt nanoparticles supported on meso-and microporous carbons for fuel cells. *Energy Fuels* **2010**, *24*, 3727–3732.
238. Yu, M.; Han, Y.; Li, J.; Wang, L. One-step synthesis of sodium carboxymethyl cellulose-derived carbon aerogel/nickel oxide composites for energy storage. *Chem. Eng. J.* **2017**, *324*, 287–295.
239. Han, S.; Sun, Q.; Zheng, H.; Li, J.; Jin, C. Green and facile fabrication of carbon aerogels from cellulose-based waste newspaper for solving organic pollution. *Carbohydr. Polym.* **2016**, *136*, 95–100.
240. Chen, Y.; Zhang, L.; Yang, Y.; Pang, B.; Xu, W.; Duan, G.; Jiang, S.; Zhang, K. Recent progress on nanocellulose aerogels: Preparation, modification, composite fabrication, applications. *Adv. Mater.* **2021**, *33*, 2005569.
241. Antolini, E. Lignocellulose, cellulose and lignin as renewable alternative fuels for direct biomass fuel cells. *ChemSusChem* **2021**, *14*, 189–207.
242. Cheng, S.; Rettew, R.E.; Sauerbrey, M.; Alamgir, F.M. Architecture-dependent surface chemistry for Pt monolayers on carbon-supported Au. *ACS Appl. Mater. Interfaces* **2011**, *3*, 3948–3956.

243. Park, S.J.; Kim, B.J.; Lee, S.Y. Effect of surface modification of mesoporous carbon supports on the electrochemical activity of fuel cells. *J. Colloid Interface Sci.* **2013**, *405*, 150–156.
244. Su, F.; Tian, Z.; Poh, C.K.; Wang, Z.; Lim, S.H.; Liu, Z.; Lin, J. Pt nanoparticles supported on nitrogen-doped porous carbon nanospheres as an electrocatalyst for fuel cells. *Chem. Mater.* **2010**, *22*, 832–839.
245. Harzer, G.S.; Orfanidi, A.; El-Sayed, H.; Madkikar, P.; Gasteiger, H.A. Tailoring catalyst morphology towards high performance for low Pt loaded PEMFC cathodes. *J. Electrochem. Soc.* **2018**, *165*, F770.
246. Saifuddin, N.; Raziah, A.; Junizah, A. Carbon Nanotubes: A Review on Structure and Their Interaction with Proteins. *J. Chem.* **2013**, *2013*, 676815. doi:10.1155/2013/676815.
247. Planeix, J.; Coustel, N.; Coq, B.; Brotons, V.; Kumbhar, P.; Dutartre, R.; Geneste, P.; Bernier, P.; Ajayan, P. Application of carbon nanotubes as supports in heterogeneous catalysis. *J. Am. Chem. Soc.* **1994**, *116*, 7935–7936.
248. Brandao, A.T.; Rosoiu, S.; Costa, R.; Lazar, O.A.; Silva, A.F.; Anicai, L.; Pereira, C.M.; Enachescu, M. Characterization and electrochemical studies of MWCNTs decorated with Ag nanoparticles through pulse reversed current electrodeposition using a deep eutectic solvent for energy storage applications. *J. Mater. Res. Technol.* **2021**, *15*, 342–359.
249. Ohtaka, A.; Sansano, J.M.; Nájera, C.; Miguel-García, I.; Berenguer-Murcia, Á.; Cazorla-Amorós, D. Palladium and Bimetallic Palladium–Nickel Nanoparticles Supported on Multiwalled Carbon Nanotubes: Application to Carbon-Carbon Bond-Forming Reactions in Water. *ChemCatChem* **2015**, *7*, 1841–1847.
250. Li, Y.; Fu, Y.; Lai, C.; Qin, L.; Li, B.; Liu, S.; Yi, H.; Xu, F.; Li, L.; Zhang, M.; et al. Porous materials confining noble metals for the catalytic reduction of nitroaromatics: Controllable synthesis and enhanced mechanism. *Environ. Sci.-Nano* **2021**, *8*, 3067–3097.
251. Guo, D.J.; Cui, S.K. A composite strategy to prepare high active Pt-WO3/MWCNT catalysts for methanol electro-oxidation. *J. Phys. Chem. Solids* **2021**, *159*, 110293.
252. Lee, K.M.; Li, L.; Dai, L. Asymmetric end-functionalization of multi-walled carbon nanotubes. *J. Am. Chem. Soc.* **2005**, *127*, 4122–4123.
253. De Volder, M.F.; Tawfick, S.H.; Baughman, R.H.; Hart, A.J. Carbon nanotubes: Present and future commercial applications. *Science* **2013**, *339*, 535–539.
254. Li, Y.; Hu, F.P.; Wang, X.; Shen, P.K. Anchoring metal nanoparticles on hydrofluoric acid treated multiwalled carbon nanotubes as stable electrocatalysts. *Electrochem. Commun.* **2008**, *10*, 1101–1104.
255. Wang, Z.; Zhang, Q.; Kuehner, D.; Ivaska, A.; Niu, L. Green synthesis of 1–2 nm gold nanoparticles stabilized by amine-terminated ionic liquid and their electrocatalytic activity in oxygen reduction. *Green Chem.* **2008**, *10*, 907–909.
256. Tunckol, M.; Fantini, S.; Malbosc, F.; Durand, J.; Serp, P. Effect of the synthetic strategy on the non-covalent functionalization of multi-walled carbon nanotubes with polymerized ionic liquids. *Carbon* **2013**, *57*, 209–216.
257. Zheng, M.; Li, P.; Fu, G.; Chen, Y.; Zhou, Y.; Tang, Y.; Lu, T. Efficient anchorage of highly dispersed and ultrafine palladium nanoparticles on the water-soluble phosphonate functionalized multiwall carbon nanotubes. *Appl. Catal. B Environ.* **2013**, *129*, 394–402.
258. Maya-Cornejo, J.; Garcia-Bernabé, A.; Compañ, V. Bimetallic Pt-M electrocatalysts supported on single-wall carbon nanotubes for hydrogen and methanol electrooxidation in fuel cells applications. *Int. J. Hydrogen Energy* **2018**, *43*, 872–884.
259. Bhuvanendran, N.; Ravichandran, S.; Zhang, W.; Ma, Q.; Xu, Q.; Khotseng, L.; Su, H. Highly efficient methanol oxidation on durable PtxIr/MWCNT catalysts for direct methanol fuel cell applications. *Int. J. Hydrogen Energy* **2020**, *45*, 6447–6460.
260. Yu, D.; Xue, Y.; Dai, L. Vertically aligned carbon nanotube arrays co-doped with phosphorus and nitrogen as efficient metal-free electrocatalysts for oxygen reduction. *J. Phys. Chem. Lett.* **2012**, *3*, 2863–2870.
261. Jin, Z.; Nie, H.; Yang, Z.; Zhang, J.; Liu, Z.; Xu, X.; Huang, S. Metal-free selenium doped carbon nanotube/graphene networks as a synergistically improved cathode catalyst for oxygen reduction reaction. *Nanoscale* **2012**, *4*, 6455–6460.
262. Sumpter, B.G.; Meunier, V.; Romo-Herrera, J.M.; Cruz-Silva, E.; Cullen, D.A.; Terrones, H.; Smith, D.J.; Terrones, M. Nitrogen-mediated carbon nanotube growth: Diameter reduction, metallicity, bundle dispersability, and bamboo-like structure formation. *ACS Nano* **2007**, *1*, 369–375.
263. Chizari, K.; Janowska, I.; Houllé, M.; Florea, I.; Ersen, O.; Romero, T.; Bernhardt, P.; Ledoux, M.J.; Pham-Huu, C. Tuning of nitrogen-doped carbon nanotubes as catalyst support for liquid-phase reaction. *Appl. Catal. A Gen.* **2010**, *380*, 72–80.
264. Chen, G.X.; Zhang, J.M.; Wang, D.D.; Xu, K.W. First-principles study of palladium atom adsorption on the boron- or nitrogen-doped carbon nanotubes. *Phys. B Condens. Matter* **2009**, *404*, 4173–4177. doi:10.1016/j.physb.2009.07.182.
265. Rajala, T.; Kronberg, R.; Backhouse, R.; Buan, M.E.M.; Tripathi, M.; Zitolo, A.; Jiang, H.; Laasonen, K.; Susi, T.; Jaouen, F.; et al. A platinum nanowire electrocatalyst on single-walled carbon nanotubes to drive hydrogen evolution. *Appl. Catal. B Environ.* **2020**, *265*, 118582.
266. Tsai, M.C.; Yeh, T.K.; Tsai, C.H. An improved electrodeposition technique for preparing platinum and platinum–ruthenium nanoparticles on carbon nanotubes directly grown on carbon cloth for methanol oxidation. *Electrochem. Commun.* **2006**, *8*, 1445–1452.
267. Zhang, l.; Fang, Z.; Zhao, G.C.; Wei, X.W. Electrodeposited Platinum Nanoparticles on the Multi-Walled Carbon Nanotubes and its Electrocatalytic for Nitric Oxide. *Int. J. Electrochem. Sci.* **2008**, *3*, 746–754.
268. Chen, X.; Li, N.; Eckhard, K.; Stoica, L.; Xia, W.; Assmann, J.; Muhler, M.; Schuhmann, W. Pulsed electrodeposition of Pt nanoclusters on carbon nanotubes modified carbon materials using diffusion restricting viscous electrolytes. *Electrochem. Commun.* **2007**, *9*, 1348–1354. doi:10.1016/j.elecom.2007.01.034.

269. Xiao, F.; Mo, Z.; Zhao, F.; Zeng, B. Ultrasonic-electrodeposition of gold–platinum alloy nanoparticles on multi-walled carbon nanotubes – ionic liquid composite film and their electrocatalysis towards the oxidation of nitrite. *Electrochem. Commun.* **2008**, *10*, 1740–1743. doi:10.1016/j.elecom.2008.09.004.
270. Huang, J.; Xie, Q.; Tan, Y.; Fu, Y.; Su, Z.; Huang, Y.; Yao, S. Preparation of Pt/multiwalled carbon nanotubes modified Au electrodes via Pt–Cu co-electrodeposition/Cu stripping protocol for high-performance electrocatalytic oxidation of methanol. *Mater. Chem. Phys.* **2009**, *118*, 371–378. doi:10.1016/j.matchemphys.2009.08.006.
271. Lorençon, E.; Ferlauto, A.S.; de Oliveira, S.; Miquita, D.R.; Resende, R.R.; Lacerda, R.G.; Ladeira, L.O. Direct production of carbon nanotubes/metal nanoparticles hybrids from a redox reaction between metal ions and reduced carbon nanotubes. *ACS Appl. Mater. Interfaces* **2009**, *1*, 2104–2106.
272. Huang, J.Y.; Ding, F.; Yakobson, B.I.; Lu, P.; Qi, L.; Li, J. In situ observation of graphene sublimation and multi-layer edge reconstructions. *Proc. Natl. Acad. Sci. USA* **2009**, *106*, 10103–10108.
273. Zhu, Y.; Murali, S.; Cai, W.; Li, X.; Suk, J.W.; Potts, J.R.; Ruoff, R.S. Correction: Graphene and Graphene Oxide: Synthesis, Properties, and Applications. *Adv. Mater.* **2010**, *22*, 5226–5226.
274. Liu, M.; Hof, F.; Moro, M.; Valenti, G.; Paolucci, F.; Pénicaud, A. Carbon supported noble metal nanoparticles as efficient catalysts for electrochemical water splitting. *Nanoscale* **2020**, *12*, 20165–20170.
275. Yang, N.; Swain, G.M.; Jiang, X. Nanocarbon electrochemistry and electroanalysis: Current status and future perspectives. *Electroanalysis* **2016**, *28*, 27–34.
276. Huang, X.; Yin, Z.; Wu, S.; Qi, X.; He, Q.; Zhang, Q.; Yan, Q.; Boey, F.; Zhang, H. Graphene-based materials: Synthesis, characterization, properties, and applications. *Small* **2011**, *7*, 1876–1902.
277. Huang, X.; Qi, X.; Boey, F.; Zhang, H. Graphene-based composites. *Chem. Soc. Rev.* **2012**, *41*, 666–686.
278. Li, X.; Cai, W.; An, J.; Kim, S.; Nah, J.; Yang, D.; Piner, R.; Velamakanni, A.; Jung, I.; Tutuc, E.; et al. Large-Area Synthesis of High-Quality and Uniform Graphene Films on Copper Foils. *Science* **2009**, *324*, 1312–1314. doi:10.1126/science.1171245.
279. Lotya, M.; Hernandez, Y.; King, P.J.; Smith, R.J.; Nicolosi, V.; Karlsson, L.S.; Blighe, F.M.; De, S.; Wang, Z.; McGovern, I.T.; et al. Liquid Phase Production of Graphene by Exfoliation of Graphite in Surfactant/Water Solutions. *J. Am. Chem. Soc.* **2009**, *131*, 3611–3620. doi:10.1021/ja807449u.
280. Farooqui, U.; Ahmad, A.; Hamid, N. Graphene oxide: A promising membrane material for fuel cells. *Renew. Sustain. Energy Rev.* **2018**, *82*, 714–733.
281. Arukula, R.; Vinothkannan, M.; Kim, A.R.; Yoo, D.J. Cumulative effect of bimetallic alloy, conductive polymer and graphene toward electrooxidation of methanol: An efficient anode catalyst for direct methanol fuel cells. *J. Alloy. Compd.* **2019**, *771*, 477–488.
282. Su, C.; Loh, K.P. Carbocatalysts: Graphene Oxide and Its Derivatives. *Accounts Chem. Res.* **2013**, *46*, 2275–2285. doi:10.1021/ar300118v.
283. Zhao, H.; Yang, J.; Wang, L.; Tian, C.; Jiang, B.; Fu, H. Fabrication of a palladium nanoparticle/graphene nanosheet hybrid via sacrifice of a copper template and its application in catalytic oxidation of formic acid. *Chem. Commun.* **2011**, *47*, 2014–2016.
284. Chen, X.; Wu, G.; Chen, J.; Chen, X.; Xie, Z.; Wang, X. Synthesis of "clean" and well-dispersive Pd nanoparticles with excellent electrocatalytic property on graphene oxide. *J. Am. Chem. Soc.* **2011**, *133*, 3693–3695.
285. Chen, Y.; Yang, X.; Kitta, M.; Xu, Q. Monodispersed Pt nanoparticles on reduced graphene oxide by a non-noble metal sacrificial approach for hydrolytic dehydrogenation of ammonia borane. *Nano Res.* **2017**, *10*, 3811–3816.
286. Jeong, D.W.; Park, S.; Choi, W.J.; Bae, G.; Chung, Y.J.; Yang, C.S.; Lee, Y.K.; Kim, J.J.; Park, N.; Lee, J.O. Electron-transfer transparency of graphene: Fast reduction of metal ions on graphene-covered donor surfaces. *Phys. Status Solidi RRL* **2015**, *9*, 180–186.
287. Iqbal, M.; Li, C.; Jiang, B.; Hossain, M.S.A.; Islam, M.T.; Henzie, J.; Yamauchi, Y. Tethering mesoporous Pd nanoparticles to reduced graphene oxide sheets forms highly efficient electrooxidation catalysts. *J. Mater. Chem. A* **2017**, *5*, 21249–21256.
288. Li, S.S.; Zheng, J.N.; Ma, X.; Hu, Y.Y.; Wang, A.J.; Chen, J.R.; Feng, J.J. Facile synthesis of hierarchical dendritic PtPd nanogarlands supported on reduced graphene oxide with enhanced electrocatalytic properties. *Nanoscale* **2014**, *6*, 5708–5713.
289. Vilian, A.E.; Hwang, S.K.; Kwak, C.H.; Oh, S.Y.; Kim, C.Y.; Lee, G.w.; Lee, J.B.; Huh, Y.S.; Han, Y.K. Pt-Au bimetallic nanoparticles decorated on reduced graphene oxide as an excellent electrocatalysts for methanol oxidation. *Synth. Met.* **2016**, *219*, 52–59.
290. Hassan, H.M.; Abdelsayed, V.; Abd El Rahman, S.K.; AbouZeid, K.M.; Terner, J.; El-Shall, M.S.; Al-Resayes, S.I.; El-Azhary, A.A. Microwave synthesis of graphene sheets supporting metal nanocrystals in aqueous and organic media. *J. Mater. Chem.* **2009**, *19*, 3832–3837.
291. Bai, R.G.; Muthoosamy, K.; Zhou, M.; Ashokkumar, M.; Huang, N.M.; Manickam, S. Sonochemical and sustainable synthesis of graphene-gold (G-Au) nanocomposites for enzymeless and selective electrochemical detection of nitric oxide. *Biosens. Bioelectron.* **2017**, *87*, 622–629.
292. Huang, Y.X.; Xie, J.F.; Zhang, X.; Xiong, L.; Yu, H.Q. Reduced graphene oxide supported palladium nanoparticles via photoassisted citrate reduction for enhanced electrocatalytic activities. *ACS Appl. Mater. Interfaces* **2014**, *6*, 15795–15801.
293. Zhou, X.; Huang, X.; Qi, X.; Wu, S.; Xue, C.; Boey, F.Y.C.; Yan, Q.; Chen, P.; Zhang, H. In Situ Synthesis of Metal Nanoparticles on Single-Layer Graphene Oxide and Reduced Graphene Oxide Surfaces. *J. Phys. Chem. C* **2009**, *113*, 10842–10846. doi:10.1021/jp903821n.
294. Qin, X.; Li, Q.; Asiri, A.M.; Al-Youbi, A.O.; Sun, X. One-pot synthesis of Au nanoparticles/reduced graphene oxide nanocomposites and their application for electrochemical H_2O_2, glucose, and hydrazine sensing. *Gold Bull.* **2014**, *47*, 3–8.

295. Yang, M.Q.; Pan, X.; Zhang, N.; Xu, Y.J. A facile one-step way to anchor noble metal (Au, Ag, Pd) nanoparticles on a reduced graphene oxide mat with catalytic activity for selective reduction of nitroaromatic compounds. *CrystEngComm* **2013**, *15*, 6819–6828.
296. Zou, C.; Yang, B.; Bin, D.; Wang, J.; Li, S.; Yang, P.; Wang, C.; Shiraishi, Y.; Du, Y. Electrochemical synthesis of gold nanoparticles decorated flower-like graphene for high sensitivity detection of nitrite. *J. Colloid Interface Sci.* **2017**, *488*, 135–141.
297. Liu, S.; Tian, N.; Xie, A.Y.; Du, J.H.; Xiao, J.; Liu, L.; Sun, H.Y.; Cheng, Z.Y.; Zhou, Z.Y.; Sun, S.G. Electrochemically seed-mediated synthesis of sub-10 nm tetrahexahedral Pt nanocrystals supported on graphene with improved catalytic performance. *J. Am. Chem. Soc.* **2016**, *138*, 5753–5756.
298. Sheng, H.; Wei, M.; D'Aloia, A.; Wu, G. Heteroatom polymer-derived 3D high-surface-area and mesoporous graphene sheet-like carbon for supercapacitors. *ACS Appl. Mater. Interfaces* **2016**, *8*, 30212–30224.
299. Luo, L.; Fu, C.; Yang, F.; Li, X.; Jiang, F.; Guo, Y.; Zhu, F.; Yang, L.; Shen, S.; Zhang, J. Composition-graded Cu–Pd nanospheres with Ir-doped surfaces on N-doped porous graphene for highly efficient ethanol electro-oxidation in alkaline media. *ACS Catal.* **2019**, *10*, 1171–1184.
300. Qiu, X.; Yan, X.; Cen, K.; Sun, D.; Xu, L.; Tang, Y. Achieving highly electrocatalytic performance by constructing holey reduced graphene oxide hollow nanospheres sandwiched by interior and exterior platinum nanoparticles. *ACS Appl. Energy Mater.* **2018**, *1*, 2341–2349.
301. Kumar, R.; Oh, J.H.; Kim, H.J.; Jung, J.H.; Jung, C.H.; Hong, W.G.; Kim, H.J.; Park, J.Y.; Oh, I.K. Nanohole-structured and palladium-embedded 3D porous graphene for ultrahigh hydrogen storage and CO oxidation multifunctionalities. *ACS Nano* **2015**, *9*, 7343–7351.
302. Kumar, R.; Singh, R.K.; Vaz, A.R.; Savu, R.; Moshkalev, S.A. Self-assembled and one-step synthesis of interconnected 3D network of Fe3O4/reduced graphene oxide nanosheets hybrid for high-performance supercapacitor electrode. *ACS Appl. Mater. Interfaces* **2017**, *9*, 8880–8890.
303. Qiu, X.; Li, T.; Deng, S.; Cen, K.; Xu, L.; Tang, Y. A General Strategy for the Synthesis of PtM (M= Fe, Co, Ni) Decorated Three-Dimensional Hollow Graphene Nanospheres for Efficient Methanol Electrooxidation. *Chem.–A Eur. J.* **2018**, *24*, 1246–1252.
304. Yao, C.; Zhang, Q.; Su, Y.; Xu, L.; Wang, H.; Liu, J.; Hou, S. Palladium nanoparticles encapsulated into hollow N-doped graphene microspheres as electrocatalyst for ethanol oxidation reaction. *ACS Appl. Nano Mater.* **2019**, *2*, 1898–1908.
305. Yu, K.; Lin, Y.; Fan, J.; Li, Q.; Shi, P.; Xu, Q.; Min, Y. Ternary N, S, and P-doped hollow carbon spheres derived from polyphosphazene as Pd supports for ethanol oxidation reaction. *Catalysts* **2019**, *9*, 114.
306. Zhang, H.; Liu, G.; Shi, L.; Ye, J. Single-atom catalysts: Emerging multifunctional materials in heterogeneous catalysis. *Adv. Energy Mater.* **2018**, *8*, 1701343.
307. Liu, J.; Ma, Q.; Huang, Z.; Liu, G.; Zhang, H. Recent progress in graphene-based noble-metal nanocomposites for electrocatalytic applications. *Adv. Mater.* **2019**, *31*, 1800696.
308. Stambula, S.; Gauquelin, N.; Bugnet, M.; Gorantla, S.; Turner, S.; Sun, S.; Liu, J.; Zhang, G.; Sun, X.; Botton, G.A. Chemical structure of nitrogen-doped graphene with single platinum atoms and atomic clusters as a platform for the PEMFC electrode. *J. Phys. Chem. C* **2014**, *118*, 3890–3900.
309. Yan, H.; Cheng, H.; Yi, H.; Lin, Y.; Yao, T.; Wang, C.; Li, J.; Wei, S.; Lu, J. Single-atom Pd1/graphene catalyst achieved by atomic layer deposition: Remarkable performance in selective hydrogenation of 1, 3-butadiene. *J. Am. Chem. Soc.* **2015**, *137*, 10484–10487.
310. Detavernier, C.; Dendooven, J.; Sree, S.P.; Ludwig, K.F.; Martens, J.A. Tailoring nanoporous materials by atomic layer deposition. *Chem. Soc. Rev.* **2011**, *40*, 5242–5253.
311. Sun, S.; Zhang, G.; Gauquelin, N.; Chen, N.; Zhou, J.; Yang, S.; Chen, W.; Meng, X.; Geng, D.; Banis, M.N.; et al. Single-atom catalysis using Pt/graphene achieved through atomic layer deposition. *Sci. Rep.* **2013**, *3*, 1–9.
312. Yan, H.; Lin, Y.; Wu, H.; Zhang, W.; Sun, Z.; Cheng, H.; Liu, W.; Wang, C.; Li, J.; Huang, X.; et al. Bottom-up precise synthesis of stable platinum dimers on graphene. *Nat. Commun.* **2017**, *8*, 1070.
313. Bulushev, D.A.; Zacharska, M.; Lisitsyn, A.S.; Podyacheva, O.Y.; Hage, F.S.; Ramasse, Q.M.; Bangert, U.; Bulusheva, L.G. Single atoms of Pt-group metals stabilized by N-doped carbon nanofibers for efficient hydrogen production from formic acid. *ACS Catal.* **2016**, *6*, 3442–3451.
314. Zhang, C.; Sha, J.; Fei, H.; Liu, M.; Yazdi, S.; Zhang, J.; Zhong, Q.; Zou, X.; Zhao, N.; Yu, H.; et al. Single-atomic ruthenium catalytic sites on nitrogen-doped graphene for oxygen reduction reaction in acidic medium. *ACS Nano* **2017**, *11*, 6930–6941.
315. Choi, C.H.; Kim, M.; Kwon, H.C.; Cho, S.J.; Yun, S.; Kim, H.T.; Mayrhofer, K.J.; Kim, H.; Choi, M. Tuning selectivity of electrochemical reactions by atomically dispersed platinum catalyst. *Nat. Commun.* **2016**, *7*, 10922.